SINGLE LAYER PERMITTIVITY EXTRACTION FROM MULTILAYERED BIAXIAL ANISOTROPIC MEDIA USING A RECTANGULAR WAVEGUIDE

THESIS

Benjamin I. Fogarty, Capt, USAF

AFIT-ENG-MS-17-M-028

DEPARTMENT OF THE AIR FORCE
AIR UNIVERSITY

AIR FORCE INSTITUTE OF TECHNOLOGY

Wright-Patterson Air Force Base, Ohio

AFIT-ENG-MS-17-M-028

SINGLE LAYER PERMITTIVITY EXTRACTION FROM MULTILAYERED BIAXIAL ANISOTROPIC MEDIA USING A RECTANGULAR WAVEGUIDE

THESIS

Presented to the Faculty

Department of Electrical & Computer Engineering

Graduate School of Engineering and Management

Air Force Institute of Technology

Air University

Air Education and Training Command

in Partial Fulfillment of the Requirements for the

Degree of Master of Science in Electrical Engineering

Benjamin I. Fogarty, B.S.E.E.

Capt, USAF

March 23, 2017

AFIT-ENG-MS-17-M-028

SINGLE LAYER PERMITTIVITY EXTRACTION FROM MULTILAYERED BIAXIAL ANISOTROPIC MEDIA USING A RECTANGULAR WAVEGUIDE

THESIS

Benjamin I. Fogarty, B.S.E.E.
Capt, USAF

Committee Membership:

Dr. Michael J. Havrilla
Chair

Dr. Peter J. Collins
Member

Lt Col Milo W. Hyde, PhD
Member

AFIT-ENG-MS-17-M-028

Abstract

Electromagnetic characterization of layered biaxial media is a critical step in the design of modern low observable (LO) coatings, and with the advent of 3D printing technology it is now possible to design and create myriad different such materials. Biaxial materials are of specific interest due to the flexibility they provide for control over magnitude, phase, and polarization of the material system's response to interrogating electromagnetic (EM) energy.

This research effort, rather than being concerned with the exhaustive characterization of a material, which has been previously done, is instead concerned with empirically proving a technique for extracting the constitutive parameters $\overleftrightarrow{\epsilon}$ and $\overleftrightarrow{\mu}$ of a specific biaxial material layer from experimentally measured scattering parameters of an entire multilayered biaxial material system. Towards this aim, a rectangular waveguide is used with several composite and plexiglass samples irradiated at X-band frequencies. The method explored in the research herein shows that the individual layers of a multilayered biaxial anisotropic dielectric material can be successfully characterized and extracted from the overall system, thus providing a valuable technique for characterizing complex layered material coatings.

For Margaret.

Acknowledgements

I would like to thank Dr. Michael Havrilla, Dr. Peter Collins and Lt Col Milo Hyde for their tireless efforts to help bring this thesis to fruition as well as their boundless insight into the topic. Furthermore, many thanks are owed to Alex Knisely for his earnest dedication to helping me achieve a foundational understanding of the topic and for this thesis' heavy reliance on his thorough work previously. Many thanks are owed to Capts Wes Petree, Joe Sciacca, Elliott Erstein, Josh Day, and Nick Zimmerman for being the best comrades in this scholastic enterprise that I could have hoped for.

Table of Contents

List of Figures

List of Tables

SINGLE LAYER PERMITTIVITY EXTRACTION FROM MULTILAYERED BIAXIAL ANISOTROPIC MEDIA USING A RECTANGULAR WAVEGUIDE

I. Introduction

1.1 Problem Statement.

The goal of this research effort is to develop a novel technique to measure the relative permittivity of individual layers of a multilayered biaxial anisotropic (BA) material. Biaxial anisotropic materials are materials characterized by having regular sub-wavelength features within the material with geometries varying in every axis that provide a controllable response to electromagnetic excitation.

A physical sample of the material is designed and printed with a 3D printer to then be inserted into an X-band (8.2-12.4 GHz) waveguide shown in Figure 1 and excited with a network analyzer. The simulated and measured data is subsequently run through a MATLAB program designed to extract S-parameters from the material system for each layer. These S-parameters correspond to reflection and transmission coefficients that enable the calculation of relative permittivity via the Nicholson-Ross-Weir (NRW) method. Since the samples are electrically thick the transmission measurement extraction will also be performed for each sample to avoid the the reflection measurement resonances from the data caused by standing waves building up in the samples themselves. Success is defined by the extracted empirical permittivity tensor for each BA layer matching the extracted empirical permittivity tensor for the individual layer found in a stand-alone test.

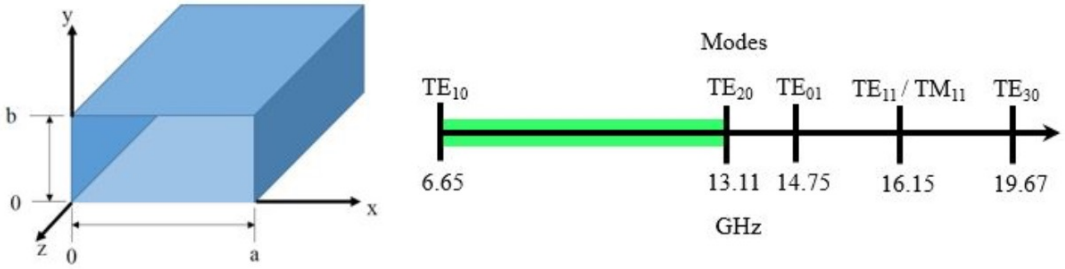

Figure 1. Rectangular Waveguide coordinate system and corresponding propagation modes for X-band [1]

1.2 Motivation & Scope.

Biaxial anisotropic materials are materials represented by $\overleftrightarrow{\epsilon}$ and $\overleftrightarrow{\mu}$ as tensors

$$\overleftrightarrow{\epsilon} = \begin{bmatrix} \epsilon_{xx} & 0 & 0 \\ 0 & \epsilon_{yy} & 0 \\ 0 & 0 & \epsilon_{zz} \end{bmatrix}, \quad \overleftrightarrow{\mu} = \begin{bmatrix} \mu_{xx} & 0 & 0 \\ 0 & \mu_{yy} & 0 \\ 0 & 0 & \mu_{zz} \end{bmatrix} \tag{1}$$

where all tensor elements are orthogonal. This leads to the physical realization of samples as polymer rectangles with the macro dimensions limited to the interior dimensions of the waveguide but with periodic orthorhombic occlusions as shown in the example in Figure 2.

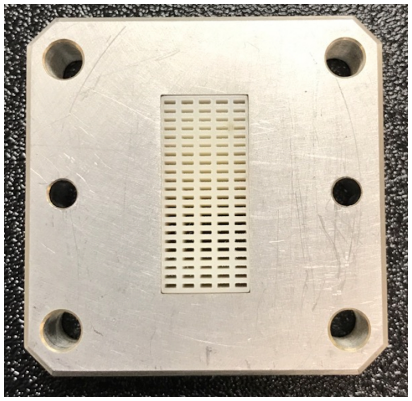

Figure 2. Biaxial anisotropic white polymer sample filling X-band waveguide sample holder

A specific application for multilayered BA materials is the skin of an aircraft, not made from traditional metallic materials, but from composite multilayered material as well that provide different effects at different depths. These effects would be designed to overcome a wide frequency range of radar signals which can penetrate to different depths in any given material.

The waveguide system is chosen to evaluate the materials under test (MUT) because the well-established Thru-Reflect-Line (TRL) calibration described in [14] can be used and measurements can be made in the simplest environment with y-invariant fields at the fundamental TE_{10} mode. This robust calibration technique accounts for systemic errors inherent to the waveguide measurement system in reflection and transmission measurements.

A variety of MUTs including isotropic, uniaxial, and biaxial are evaluated as layers of a two-layered system as well as independently to verfiy the proposed method of this research effort. Each dataset acquired from these experiments is converted from experimental S-parameters to experimental A-parameters and subsequently to ϵ_r via two methods: the Nicholson-Ross-Weir technique which exhibits a resonance caused by standing waves in the sample and through the 1-D Newton Root Search method which will remove the resonance since it is based on only transmission measurements which are nonzero (eliminating the possibility of a divide-by-zero causing a discontinuity).

1.3 Limitations and Challenges.

This thesis is confined to the X-band due to limitations of the laboratory equipment and for the purposes of proof-of-concept. Furthermore, the maximum number of layers tested is two, but the implication is that the number of layers could be infinite as the theory can be extrapolated to any number of layers. Due to the nature of the

rectangular waveguide, and the requirement for samples to fill the entire space within it to avoid exciting higher order modes [1] and maintain a closed form solution, the material samples themselves cannot be fully characterized in every orientation. To do so would require a Waveguide Rectangular to Waveguide Square (WRWS) system with cubic samples. For ease of proving the technique and reusing existing samples, the rectangular waveguide is used instead because the full characterization of a particular sample is not the primary goal, rather being able to mathematically determine a single layer's constitutive parameters as distinct from the entire layered system is more critical and a single orientation suffices.

1.4 Resource Requirements.

The Air Force Institute of Technology (AFIT) material measurements laboratory contains all of the requisite equipment including the waveguide, Vector Network Analyzer, thru, reflect and line standards for calibration, and printed biaxial and uniaxial material samples created on an ultraviolet-cured ink-jet 3D polymer printer. These samples were created by the Air Force Research Laboratory (AFRL), Sensors Directorate, Electromagnetics Research Branch. Lastly, AFIT provides the MATLAB license required to create the code used to analyze the data.

1.5 Thesis Organization.

This document describes the development of a new technique for the characterization of individual layers of layered biaxial anisotropic material measurement. Chapter 2 provides background information on biaxial anisotropic material design and characterization as well as layered analysis previously performed on isotropic media. Chapter 3 provides the theoretical background starting from Maxwell's equations for layered biaxial media in a waveguide. An exploration of the limitations of the ap-

proach of using a rectangular waveguide vs a WRWS system is discussed. Chapter 4 concerns the experiment itself, from the setup and system calibration through the various forms of processing required for achieving the desired separation of the individual layers' constitutive parameters from the whole multilayered material system. Finally, the conclusion in Chapter 5 includes an interpretation of the results in addition to suggestions for future work.

II. Background

Prior research in this area has been conducted at AFIT focusing on the design and characterization of materials in a waveguide, specifically biaxial anisotropic materials. This research effort examines several multilayered materials, each layer having a unique crystallographic symmetry, which were created using a 3D polymer printer. While both biaxial anisotropic media and layered media are by no means novel topics for examination, this is the first time they have been analyzed and characterized as part of a combined effort. To that end, this chapter provides the background on both aspects of this thesis necessary for understanding the modal analysis and material parameter extraction necessary for characterizing complex media.

2.1 History of Biaxial Anisotropic Material Measurement.

A significant effort has been made in recent years at AFIT and elsewhere to further the technical capabilities of researchers to fully characterize biaxial anistropic media. This culminated in the design and implementation of the WRWS and its application to Knisely's thesis [1]. In his thesis and a variety of other papers, Mr. Knisely and Dr. Havrilla have exercised the WRWS system using a variety of BA samples designed with different crystallographic structures as cubes that can be fully characterized in 6 orientation with a single sample, which was a noted improvement over previous techniques used by Damaskos et al [6] and Crowgey et al in [7] and [8].

In the aforementioned research the measurement procedure suggested rotating the sample within the waveguide to sufficiently characterize all tensor elements of the complex permittivity and permeability, however multiple samples were required in order to arrive at a full characterization in order to keep samples thin and because of the inherent dimensionality of a rectangular waveguide.

The next logical step in the progression towards the WRWS was using a cubic sample in a cubic sample holder [7], which poses two problems: the first is the excitation of higher modes due to the abrupt change in the waveguide aperture at the sample holder which requires a complex modal analysis instead of a closed form NRW extraction [1], and the second problem is a loss of signal strength. To overcome these problems Tang et al [8] performed experiments with cubic samples in rectangular sample holders with open cavities on either side of the centered sample. This method was also plagued by similar problems of exciting higher order modes, but did not suffer from loss of signal.

Enter the WRWS and the successful characterization of biaxial anisotropic samples using a single cubic sample in Alexander Knisely's thesis [1]. The gradual waveguide transitions prevent high order modes from being excited within the waveguide, maintaining the fundamental TE_{10} mode only, and it supports closed-form solutions for NRW extraction of the constitutive parameters of biaxial media.

Figure 3 shows the progression described in the previous paragraphs.

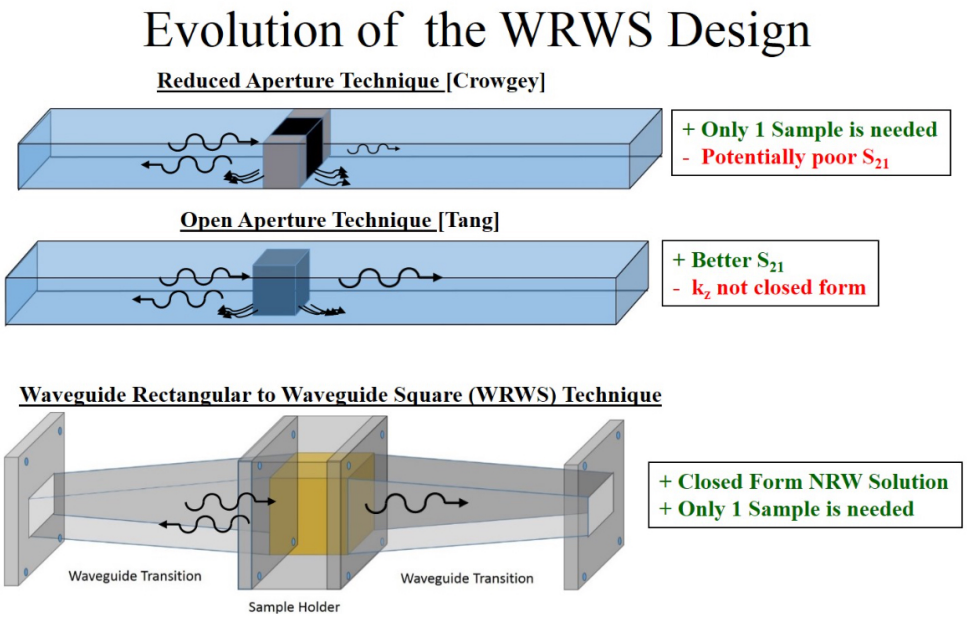

Figure 3. Evolution of the WRWS and biaxial anisotropic material characterization [1]

2.2 Characterization of Single Layer Biaxial Media.

Biaxial anisotropic materials are of interest because they provide additional degrees of freedom over isotropic materials in controlling the response of the material to interrogating EM energy. Moreover, BA materials provide an additional degree of freedom over uniaxial materials as well since uniaxial materials inherently only have two different characterizations, $\overleftrightarrow{\epsilon_t}$ and $\overleftrightarrow{\epsilon_z}$. Biaxial materials have numerous applications, but chief among them for the purposes of a thesis concerned with layered materials, are absorbers and coatings for LO applications. Therefore, understanding how to design and characterize these materials can lead to the ability to design and defeat enemy microwave detection systems. For a mathematically rigorous analysis on this topic, refer to Knisely's thesis [1].

2.3 Previous Layered Media Analysis - Isotropic.

Methods for extracting material parameters from layered media were initially researched out of a desire to characterize unknown materials prone to warping and bending, which would be attached by an adhesive to a known substrate layer. Since this work was done by Havrilla [15] and others before the advent of the WRWS, a rectangular waveguide was used. Subsequently the samples that were being tested were intentionally isotropic simple media to limit complexity of the experiment and be able to fully characterize a given sample with a single measurement. Two methods were developed in this research, known as the De-embed and Direct Methods and are discussed further in the layered analysis section of Chapter 3. This research showed that some distinctions between the results for the two methods were significant. The results of the direct method clearly showed the ability to perceive undesirable inhomogeneities in the unknown layer of the heretofore believed isotropic material. The de-embed results for the same material was not so illuminating, but instead incor-

rectly showed high levels of consistency between forward and reverse measurements. However, this failure of the de-embed method to correctly characterize poorly fabricated samples does not invalidate the method itself, but it does imply that some caution must be used when using unfamiliar and previously uncharacterized samples.

III. Biaxial Theory

3.1 Maxwellian Field Analysis for Biaxial Materials in a Rectangular Waveguide.

Initial assumptions and criteria for performing this analysis are that the waveguide environment is source-free and the fields contained within it are y-invariant. Also, all the media being evaluated is treated as though it were the most complex case, biaxial anisotropic. Uniaxial media merely has ϵ_{xx}=ϵ_{yy} (called ϵ_t for transverse) and isotropic media has ϵ_{xx}=ϵ_{yy}=ϵ_{zz}. Thus, Maxwell's equations for a source-free biaxial region are

$$\nabla \times \vec{E} = -j\omega \overleftrightarrow{\mu} \cdot \vec{H} \quad \nabla \times \vec{H} = j\omega \overleftrightarrow{\epsilon} \cdot \vec{E} \tag{2}$$

where the tensor expansions of the constitutive parameters are

$$\overleftrightarrow{\epsilon} = \begin{bmatrix} \epsilon_{xx} & 0 & 0 \\ 0 & \epsilon_{yy} & 0 \\ 0 & 0 & \epsilon_{zz} \end{bmatrix}, \quad \overleftrightarrow{\mu} = \begin{bmatrix} \mu_{xx} & 0 & 0 \\ 0 & \mu_{yy} & 0 \\ 0 & 0 & \mu_{zz} \end{bmatrix}. \tag{3}$$

To begin the development of the TE field sets within the waveguide, the curl operator $\hat{x}\frac{\partial}{\partial x} + \hat{z}\frac{\partial}{\partial z}$ (excluding the y component as the fields are y-invariant as previously noted) is applied to the standard field set $\hat{x}E_x + \hat{y}E_y + \hat{z}E_z$ and set equal to the component decomposition of Faraday's Law from Equation 2. This results in the equation

$$\hat{z}\frac{\partial E_y}{\partial x} - \hat{y}\frac{\partial E_z}{\partial x} + \hat{y}\frac{\partial E_x}{\partial z} - \hat{x}\frac{\partial E_y}{\partial z} = -\hat{x}j\omega\mu_x H_x - \hat{y}j\omega\mu_y H_y - \hat{z}j\omega\mu_z H_z, \tag{4}$$

which leads to a similar result by reciprocity for Ampere's Law.

By separating the component parts on either side of Equation 4 and setting them equal, the field sets can be separated and individually defined as shown in Table 1.

	TE_z	TM_z
$\hat{x}$	$H_x = \frac{1}{j\omega\mu_x}\frac{\partial E_y}{\partial z}$	$E_x = -\frac{1}{j\omega\epsilon_x}\frac{\partial H_y}{\partial z}$
$\hat{y}$	$-\frac{\partial H_z}{\partial x} + \frac{\partial H_x}{\partial z} - j\omega\epsilon_y E_y = 0$	$-\frac{\partial E_z}{\partial x} + \frac{\partial E_x}{\partial z} + j\omega\mu_y H_y = 0$
$\hat{z}$	$H_z = -\frac{1}{j\omega\mu_z}\frac{\partial E_y}{\partial x}$	$E_z = \frac{1}{j\omega\epsilon_x}\frac{\partial H_y}{\partial x}$

Table 1. Field sets for biaxial media in a source-free environment with y-invariant fields in a rectangular waveguide

By substitution and separation of variables through representing H_y as a product of two functions f(x) and h(z), formulas for $-k_x^2$ and $-k_z^2$ are determined to be

$$-k_x^2 = \frac{\partial^2}{\partial x^2}, \; -k_z^2 = \frac{\partial^2}{\partial x^2}, \tag{5}$$

which when plugged back into the substitution for the TM_z field sets leads to

$$k_z = \pm\sqrt{\omega^2\epsilon_x\mu_y - \frac{\epsilon_x}{\epsilon_z}k_x^2}. \tag{6}$$

These solutions describe the propagation of the forward and reverse traveling waves in biaxial anisotropic media in the parallel polarization state. By symmetry, the TE_z solutions for the perpendicular polarization state are determined to be

$$k_z = \pm\sqrt{\omega^2\epsilon_y\mu_x - \frac{\mu_x}{\mu_z}k_x^2}. \tag{7}$$

Next, by assigning standard forms of traveling waves to f(x) and h(z) in the form of

$$f(x) = A\sin(k_x x) + B\cos(k_x x)$$
$$h(z) = Ce^{-jk_z z} + Ce^{jk_z z}, \tag{8}$$

and further substituting the new generic definition for $H_y(x,z) = f(x)h(z)$ into the $\hat{x}$ and $\hat{z}$ TM_z sets some clear physical insights arise. By applying boundary conditions such that the interior walls of the waveguide are treated as perfect electric conductors (PECs), it can be generalized that

$$E_z = 0 \text{ when } x = 0 \text{ or } x = a, \text{ where } k_x = \tfrac{m\pi}{a} \text{ for } m = 0,\ 1,\ 2\ldots \text{ and}$$
$$E_x = 0 \text{ when } y = 0\ \forall\ x \text{ and } z \tag{9}$$

This results in the mathematical impossibility of TM_z modes existing in a rectangular waveguide, which means only the TE_z modes exist. Applying the same substitution and boundary condition methods discussed above, the familiar descriptions for reflection and transmission for traveling waves in biaxial media in the waveguide are found to be

$$\Gamma_n = \tfrac{Z_n + Z_{n-1}}{Z_n + Z_{n-1}}$$
$$T_n = 1 + R_n = \tfrac{2Z_n}{Z_n + Z_{n-1}} \tag{10}$$

where the impedance $Z_n = \frac{\omega\mu_{xn}}{k_{zn}}$. From here the traditional development of the NRW method can be applied to define the scattering parameters in terms of reflection and transmission. If the phase shift caused by the physical thickness of the sample is defined as $P_n = e^{-jk_{zn}d_n}$ the diagram in Figure 4 becomes a simple depiction of the wave propagation at the sample interfaces and

$$\begin{bmatrix} c_n \\ b_n \end{bmatrix} = \frac{1}{T_n P_n} \begin{bmatrix} 1 & \Gamma_n P_n^2 \\ \Gamma_n & 1 \end{bmatrix} \begin{bmatrix} c_{n+1} \\ b_{n+1} \end{bmatrix} \tag{11}$$

is the general form of the relationships between the waves at each interface such that

$$\begin{aligned} c_{n+1} &= c'_n e^{-jk_{zn}d_n} \\ b_{n+1} &= b'_n e^{jk_{zn}d_n}. \end{aligned} \tag{12}$$

This can then be extrapolated to any number of layers, which is discussed in the next section.

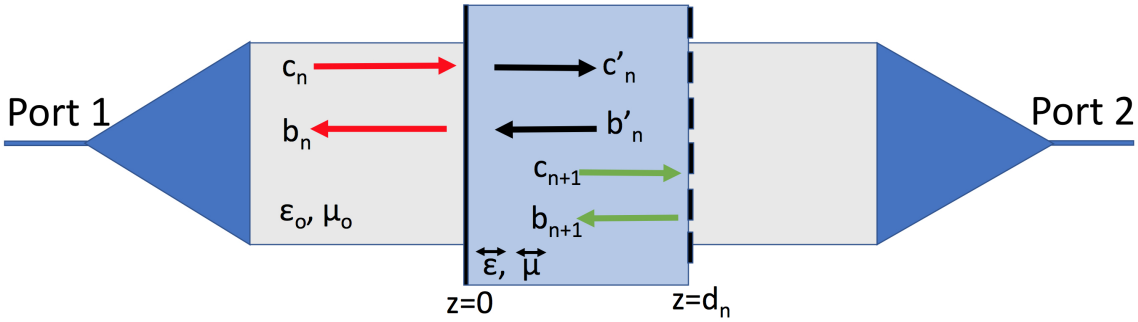

Figure 4. Generalized depiction of wave propagation in a biaxial sample in a rectangular waveguide

3.2 Layered Biaxial Media in a Rectangular Waveguide.

The traditional method for characterizing complex media via S-parameters is insufficient when the material is made of multiple layers and therefore, multiple interfaces. Therefore, in order to fully describe these systems A-parameters are used as an intermediate step to describe the signals at each interface, as opposed to the method with S-parameters which describes the signals received at each port. This can be seen in the Figure 5 and mathematically defined in the two systems described as

$$\begin{bmatrix} c_1 \\ b_1 \end{bmatrix} = \begin{bmatrix} A_{11} & A_{12} \\ A_{21} & A_{22} \end{bmatrix} \begin{bmatrix} c_3 \\ b_3 \end{bmatrix}, \text{ and } \begin{bmatrix} b_1 \\ c_3 \end{bmatrix} = \begin{bmatrix} S_{11} & S_{12} \\ S_{21} & S_{22} \end{bmatrix} \begin{bmatrix} c_1 \\ b_3 \end{bmatrix}, \tag{13}$$

which when rewritten as a system of equations, allows for the S-parameters to be solved in terms of the A-parameters, using the interface signals as the common ele-

ments. So $S_{11} = \frac{A_{21}}{A_{11}}$ and $S_{21} = \frac{1}{A_{11}}$ with similar formulas for the reverse parameters found by superposition.

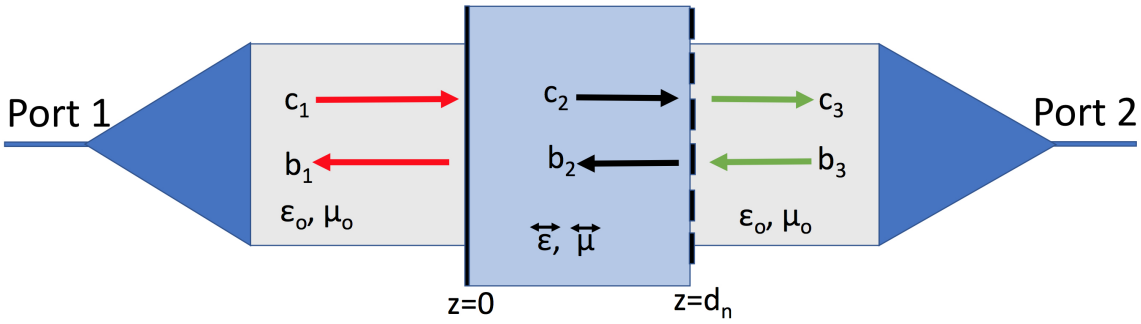

Figure 5. Generalized depiction of wave propagation in a multilayered,multi-interface biaxial system in a rectangular waveguide

Following this exercise, the A-parameters can be extrapolated to an n-layered system in familiar terms from NRW in terms of Γ_n and P_n where the nth layer can be described by

$$\begin{bmatrix} A_{11}^n & A_{12}^n \\ A_{21}^n & A_{22}^n \end{bmatrix} = \frac{1}{P_n(1-\Gamma_n^2)} \begin{bmatrix} 1-\Gamma_n^2 P_n^2 & -\Gamma_n(1-P_n)^2 \\ \Gamma_n - \Gamma_n^2 P_n^2 & -(\Gamma_n^2 - P_n^2) \end{bmatrix} \tag{14}$$

for a system described by the signals gathered at the outermost interfaces as

$$\begin{bmatrix} c_1 \\ b_1 \end{bmatrix} = \begin{bmatrix} A_{11}^{sys} & A_{12}^{sys} \\ A_{21}^{sys} & A_{22}^{sys} \end{bmatrix} \begin{bmatrix} c_{N+1} \\ b_{N+1} \end{bmatrix}, \tag{15}$$

for N layers of unique and arbitrary width.

To perform the final step and extract an unknown layer from the biaxial material system the full system can be described as the matrix product of cascading A-parameters as

$$\left[A^{sys}\right] = \left(\prod_{n=1}^{U-1}\left[A^n\right]\right)\left(\left[A^U\right]\right)\left(\prod_{n=U+1}^{N}\left[A^n\right]\right), \tag{16}$$

where A^{sys} are the A-parameters converted from the S-parameters measured with the network analyzer. Rearranging via matrix operations to solve for the unknown layer, we arrive at the final equation for the description of the unknown layer in terms of its A-parameters as

$$\left[A^U\right] = \left(\prod_{n=U-1}^{1}\left[A^n\right]^{-1}\right)\left(\left[A^{sys}\right]\right)\left(\prod_{n=N}^{U+1}\left[A^n\right]^{-1}\right), \tag{17}$$

Since S-parameters are what are typically measured, they are taken directly from the network analyzer and compared against theoretical S-parameters derived via the direct method [15]. This is accomplished by computing $[A^n]$ from empirical results for each layer separately; $[A^u]$ is calculated based on an initial guess for $\overleftrightarrow{\epsilon}_u$ and $\overleftrightarrow{\mu}_u$ using the 1-D Newton Root search. This is then converted to theoretical S-parameters. This method is used for the results in this thesis.

Alternately, $[A^n]$ is calculated, which relies on the assumption that the $\overleftrightarrow{\epsilon}_n$ and $\overleftrightarrow{\mu}_n$ are known for $n \neq U$. This can be accomplished by individually characterizing each layer one at a time as is done in this experiment. The experimentally-derived S-parameters of the whole system are converted to A-parameters, and then the unknown layer's A-parameters are extracted and converted to S-parameters. This is known as the de-embed method and uses a modified NRW extraction to compute $\overleftrightarrow{\epsilon}_u$ and $\overleftrightarrow{\mu}_u$ [15].

3.3 Incomplete $\overleftrightarrow{\epsilon}_r$ Due to Approach.

Fully characterizing BA samples is not possible with this system due to the nature of the rectangular waveguide and the requirement that samples conform to its interior dimensions in order to avoid complications from the excitation of higher order modes. Since the occlusions in each sample vary on all three orthogonal axes, a third measurement of each sample would be needed to fully characterize $\overleftrightarrow{\epsilon}_r$ and $\overleftrightarrow{\mu}_r$. Two of the samples this thesis uses have occlusions that are oriented across the shorter axis

of the sample itself and so give either ϵ_{xx} or ϵ_{yy} and both can be evaluated for ϵ_{zz}. The third biaxial sample's orthorhombic occlusions are oriented transversely with no openings visible looking down the waveguide so no longitudinal component of $\overleftrightarrow{\epsilon_r}$ (ϵ_{zz}) can be measured with this system.

It is decided that for this thesis, proving the ability to successfully extract $\overleftrightarrow{\epsilon_r}$ for a single biaxial layer of a multilayered system was paramount to full characterization of arbitrary samples. As was described in Chapter 2, Alex Knisely has previously very successfully described the process for characterizing dielectric biaxial anisotropic media in a WRWS using cubic samples that were not affected by this shortcoming.

IV. Experimental Methodology & Results

4.1 Experiment Setup.

This experiment requires a 2-port network analyzer connected to either end of an X-band waveguide. This setup provides reflection and transmission parameters from both ports. The experimental setup is shown in Figure 6 below.

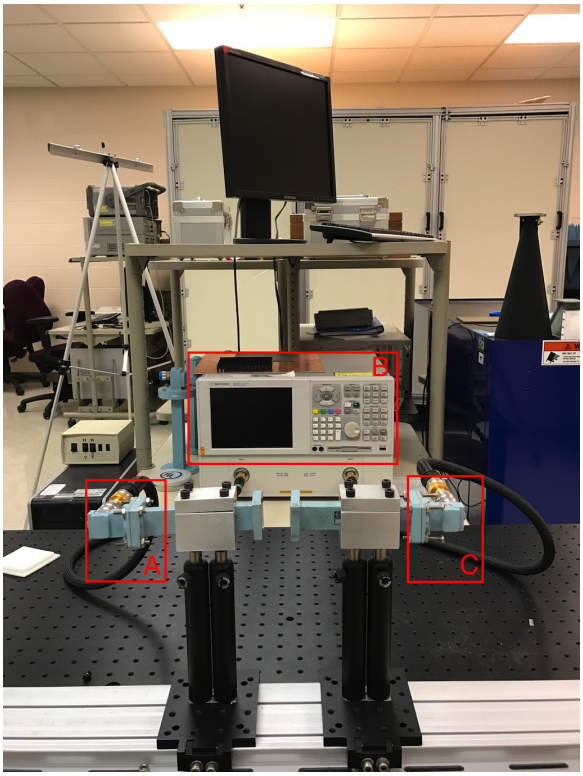

Figure 6. Experimental setup showing 2-port network analyzer (A), and waveguide system with port 1 end labeled with (B) and port 2 labeled with (C)

Before performing any experiments, the biaxial anisotropic, uniaxial, and plexiglass samples are measured for thickness. This includes width measurements of each sample and the sample holder, shown in the setup in Figure 7. The biaxial samples are the materials of primary interest as their characterization represents a new advance, but the uniaxial material will provide a simpler test case that can be fully characterized in a rectangular waveguide as both the transverse elements of its permittivity are

identical. The plexiglass layer will be used in the layered measurements as the first layer (referenced to Port 1) of all the multilayered systems. Each system will therefore be composed of two layers in the configuration: plexiglass || layer X.

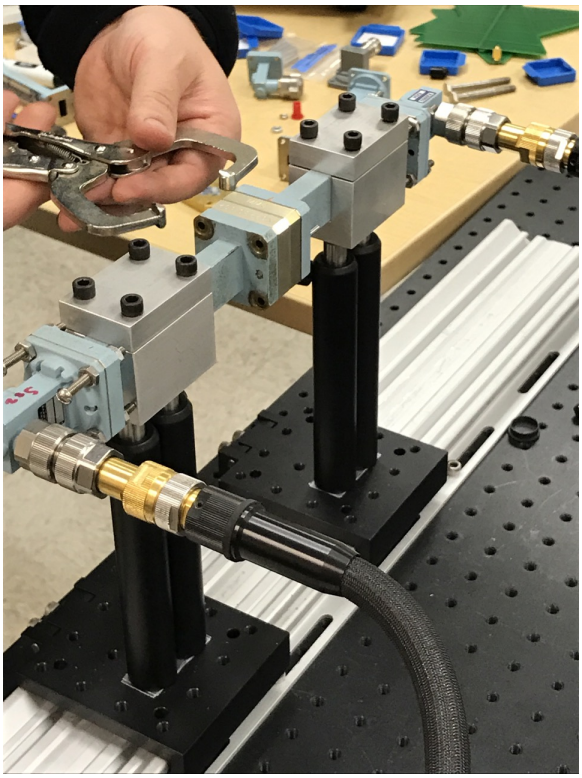

Figure 7. Experimental setup showing X-band waveguide system with a double sample holder in the measurement fixture

All of the samples have 0.9" x 0.4" edge length in order to completely fill the X-band sample holder and the BA polymer samples are measured with a digital precision micrometer as 0.3984 inches thick. The plexiglass is measured as 0.2185 inches thick and the two sample holders are measured for a combined 0.7638 inches. Two sample holders are used in series in order to accommodate the multilayered system which would extrude from a single sample holder. For the purposes of calculations of phase correction, both layered and stand-alone single layers are made flush to the left side of the double sample holders to be effectively flush to Port 1 of the network analyzer. A cutaway drawing of the experimental setup is shown in Figure 8.

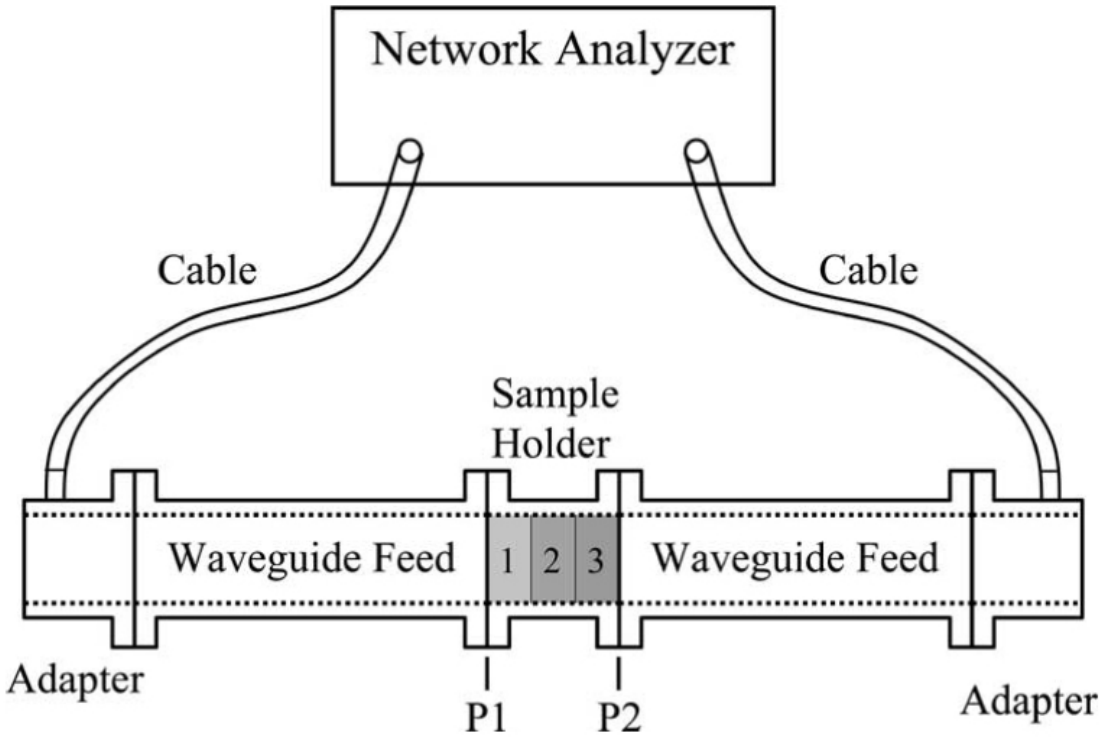

Figure 8. Cross-sectional depiction of rectangular waveguide system with layered bi-axial material in the system, region 3 marked in the diagram is always free space

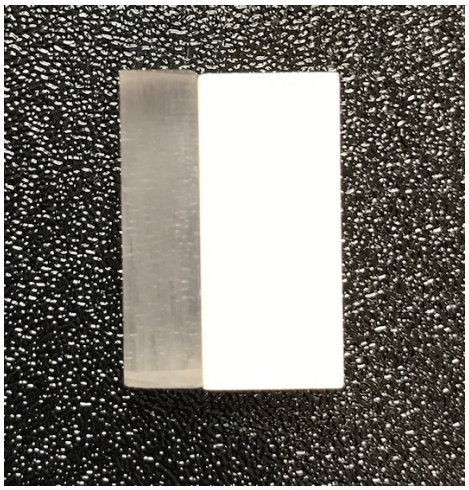

(a) Layered material system: plexiglass layer flush to a biaxial layer in test configuration

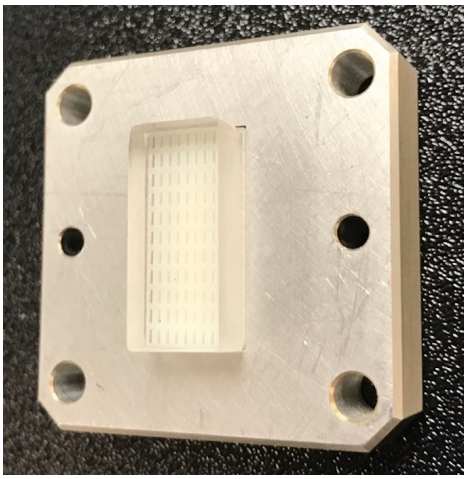

(b) Layered material system with plexiglass layer extruding from sample holder

Figure 9. Layered material systems shown from two angles to show orientation for experimentation

Each of the samples is shown below in Figure 10 loaded into a sample holder.

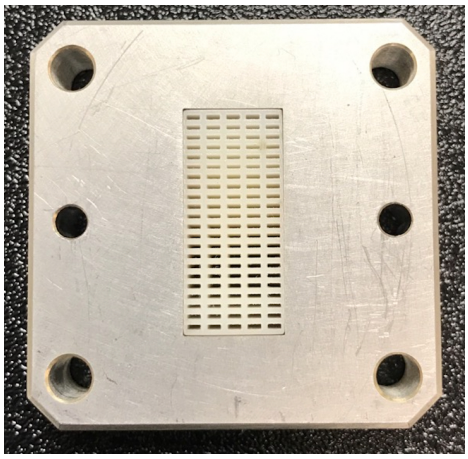

(a) Biaxial sample 1 with occlusions oriented for ϵ_{xx} measurement

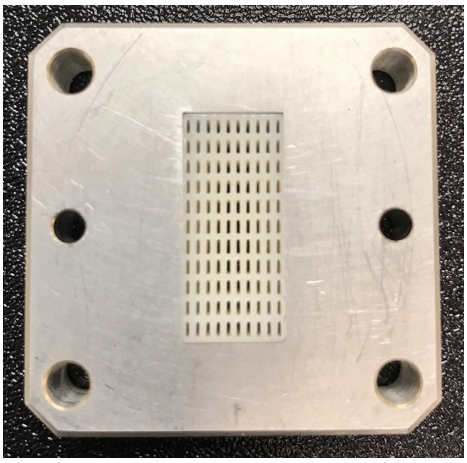

(b) Biaxial sample 2 with occlusions oriented for ϵ_{yy} measurement

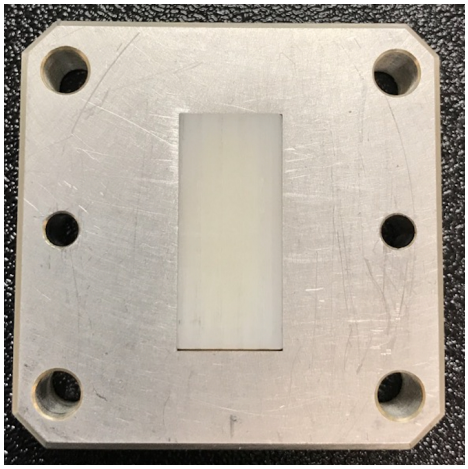

(c) Biaxial sample 3 with occlusions oriented for ϵ_{zz} measurement

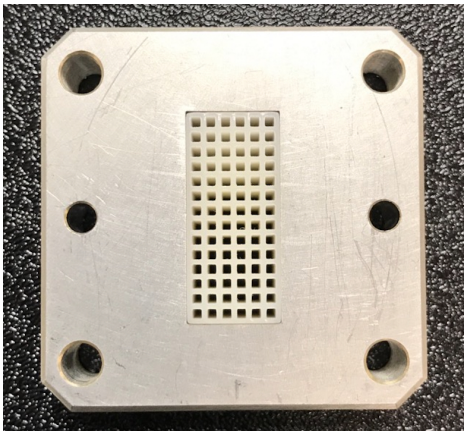

(d) Uniaxial sample with occlusions oriented for ϵ_t measurement

Figure 10. Biaxial and uniaxial samples shown in 1 test configuration each. Each sample was rotated 90° for a second measurement in another orientation

4.2 System Calibration.

After taking all the above measurements and turning on the network analyzer system, a TRL calibration is performed on the waveguide system as described by Engen and Hoer in [14] and by Rytting in [16] and [17]. First the thru measurement

is taken with the two extensions of the waveguide connected directly, with nothing between them. Following that, the reflection measurement is made with the reflection metallic short and lastly the line measurement is done with the line standard, which is the size of a single sample holder. The reflect and line standards are shown in Figure 11.

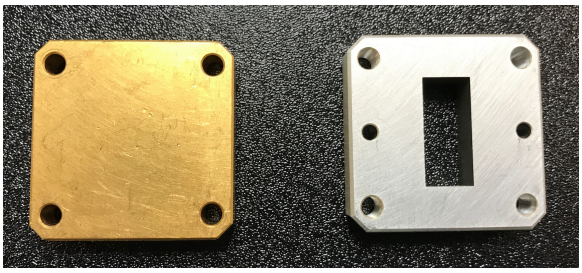

Figure 11. Reflection metallic short *(left)* and line standard *(right)*

Code is developed to perform the calibration in MATLAB based on [14] as well to validate the calibration theory, but for the sake of this experiment, the network analyzer's internal TRL calibration is used. The processing code is adapted to accept calibrated and uncalibrated measurements via a query to the user asking whether it is calibrated or not. If the answer is a 'yes', the code automatically jumps to the NRW extraction routine.

4.3 Nicholson-Ross-Weir Extraction.

The Nicolson-Ross-Weir (NRW) retrieval method for scattering parameters has been described in exhaustive detail in Alexander Knisely's thesis [1] and adapted for simple layered environments by Havrilla and Nyquist in [15]. In order to determine the forward permittivity and permeability of a given unknown layer (with matching equations for the reverse direction), the following system must be solved:

$$\begin{aligned} S_{11,sys}^{thy}(\omega, \overleftrightarrow{\epsilon}, \overleftrightarrow{\mu}) - S_{11,sys}^{exp}(\omega) = 0 \\ S_{21,sys}^{thy}(\omega, \overleftrightarrow{\epsilon}, \overleftrightarrow{\mu}) - S_{21,sys}^{exp}(\omega) = 0. \end{aligned} \tag{18}$$

In [15] Havrilla shows that expressions for theoretical S-parameters of the multilayered system ($S_{11,sys}^{thy}$,$S_{21,sys}^{thy}$) can be found using guided-wave theory in Pozar [13] using A-parameters as an intermediate step to describe the whole multilayered system. The experimental S-parameters are obtained directly via the network analyzer.

4.4 Accounting for Electrically-Thick Samples: 1-D Newton Root Search.

As is seen in the results for the permittivity extraction using the NRW technique in Figures 12 - 15, a discontinuity appears in the data at approximately 12 GHz for each sample due to the electrical thickness of the samples themselves. This discontinuity is caused by a branch cut because the sample is electrically thick when $\lambda/2 \geq$ sample thickness. These resonances occur at frequencies at which the S_{11} measurement approaches zero, resulting in singularities in the closed form solutions for permittivity and permeability [1]. From the NRW [2] method, $P = e^{-jk_z\ell_s}$ where $k_z = \frac{2\pi}{\lambda_z}$. Making the substitution leads to

$$P = e^{-j\frac{2\pi}{\lambda_z}\ell_s} = e^{-j2\pi\frac{\ell_s}{\lambda_z}}, \tag{19}$$

but if $\ell_s = \lambda/2$ then $\frac{\ell_s}{\lambda_z} = \frac{1}{2}$ and $P = e^{-j\pi} = -1$. Again from NRW,

$$S_{11} = \frac{R(1-P^2)}{1-R^2}, \tag{20}$$

but when $P = -1$, $P^2 = 1$ so $S_{11} = 0$. Finally, from NRW,

$$Q = \frac{1 + S_{11}^2 - S_{21}^2}{2\mathbf{S_{11}}}, \tag{21}$$

and R equals one of the roots of $Q \pm \sqrt{Q^2 - 1}$. Equation 21 shows that when $S_{11} = 0$, a divide-by-zero appears in the NRW method. The S_{21} measurements do not suffer this problem.

This discontinuity can be removed by applying Newton's Method, which is an iterative mathematical algorithm used to solve either of the equations in Equations System 18. Newton's Method is a mathematical device useful for numerically locating the complex roots of the equation $f(z) = 0$, where f(z) is a complex function of the variable z.

The Taylor Series expansion of $f(z + \Delta z) = 0$ is $f(z + \Delta z) \simeq f(z) + f'(z)\Delta z$, which implies

$$\Delta z = -\frac{f(z)}{f'(z)} \tag{22}$$

which can be generalized to the nth point as

$$\Delta z = z_{n+1} - z_n = -\frac{f(z_n)}{f'(z_n)}, \quad where \quad f'(z_n) \neq 0. \tag{23}$$

This gives a mathematical starting point for the Forward Problem, where instead of determining the scattering parameters directly, a non-zero guess is made for the dielectric constant ϵ, and using the method described above, a program will run the data through until a convergence is reached between the theoretical value and experimental data. The following plots should clearly elucidate the success of this technique over the direct method which is plagued by the resonance issue.

4.5 Layered Material Results.

Each of the following sets of plots shows the same data set first evaluated using the NRW method to extract the scattering parameters from the individual layers as standalone experiments and not as part of a multilayered system. The previously-mentioned discontinuity in the area of 12 GHz is readily apparent in each plot for both permeability and permittivity (only the real parts are shown here for brevity's

sake).

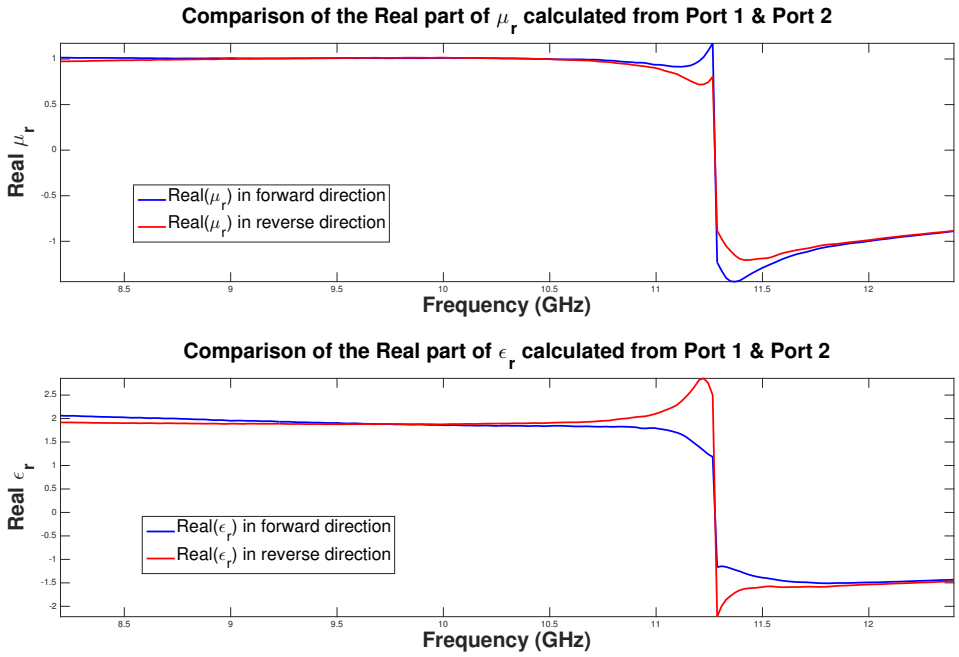

(a) Above: BA Sample 1 - Occlusions oriented to create XX-oriented $\vec{E}$ field

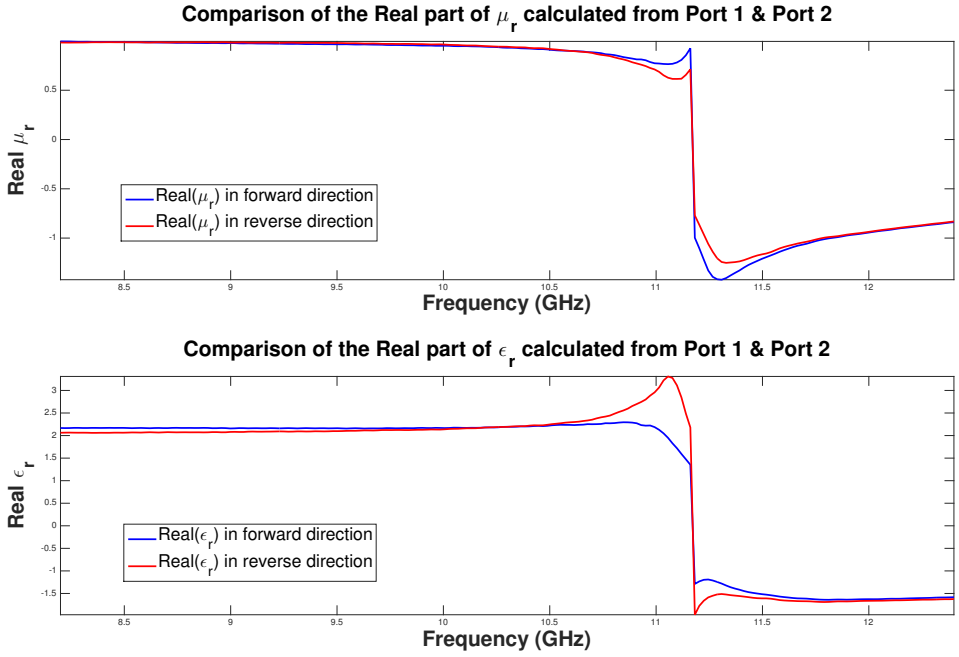

(b) Above: BA Sample 1 - Occlusions oriented to create ZZ-oriented $\vec{E}$ field

Figure 12. Biaxial sample 1 evaluated with NRW technique but no Newton root search

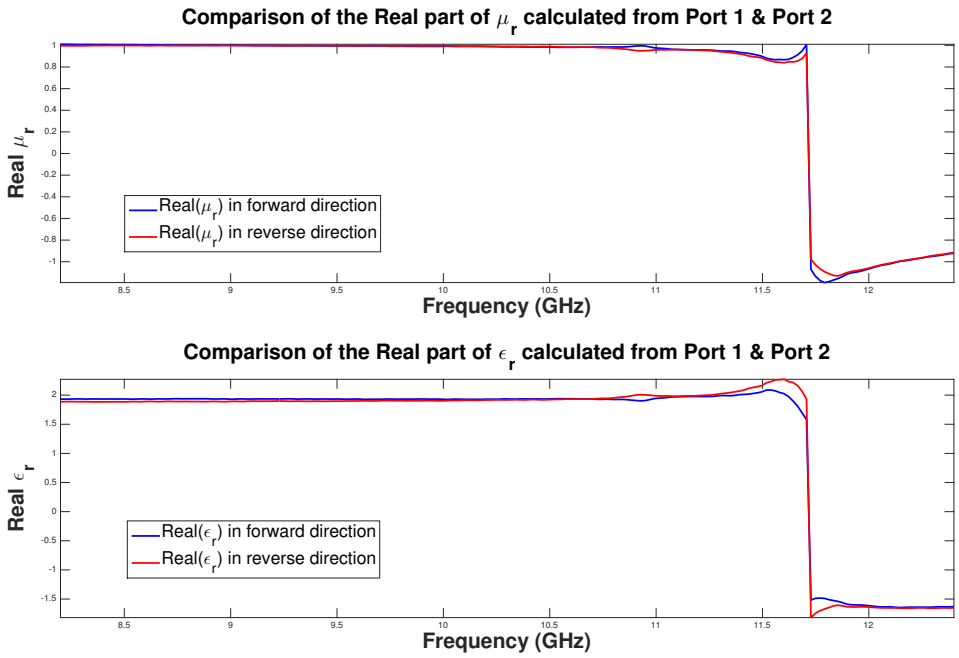

(a) Above: BA Sample 2 - Occlusions oriented to create YY-oriented $\vec{E}$ field

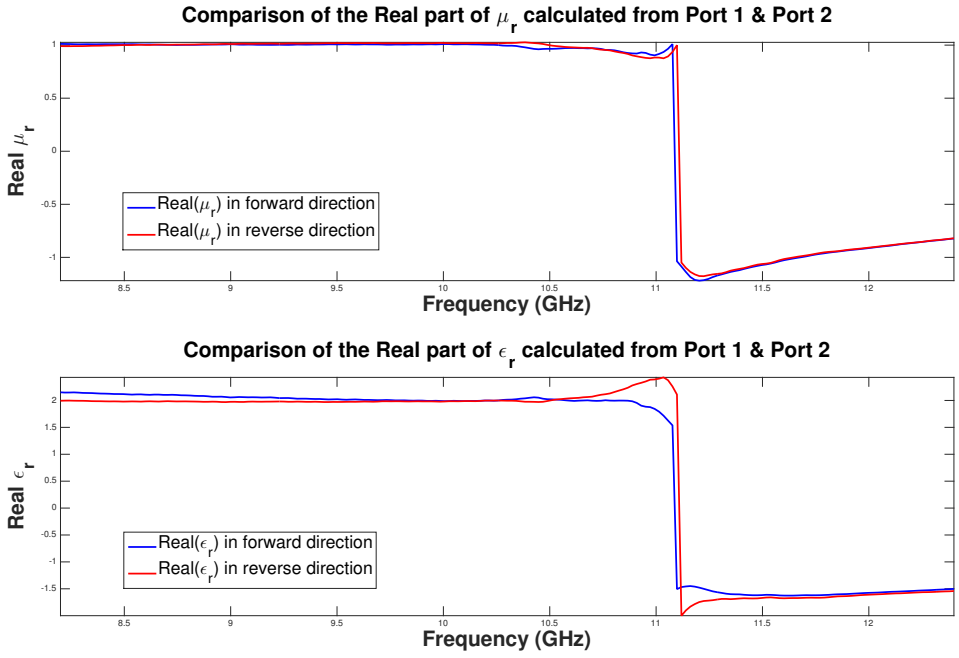

(b) Above: BA Sample 2 - Occlusions oriented to create ZZ-oriented $\vec{E}$ field

Figure 13. Biaxial sample 2 evaluated with NRW technique but no Newton root search

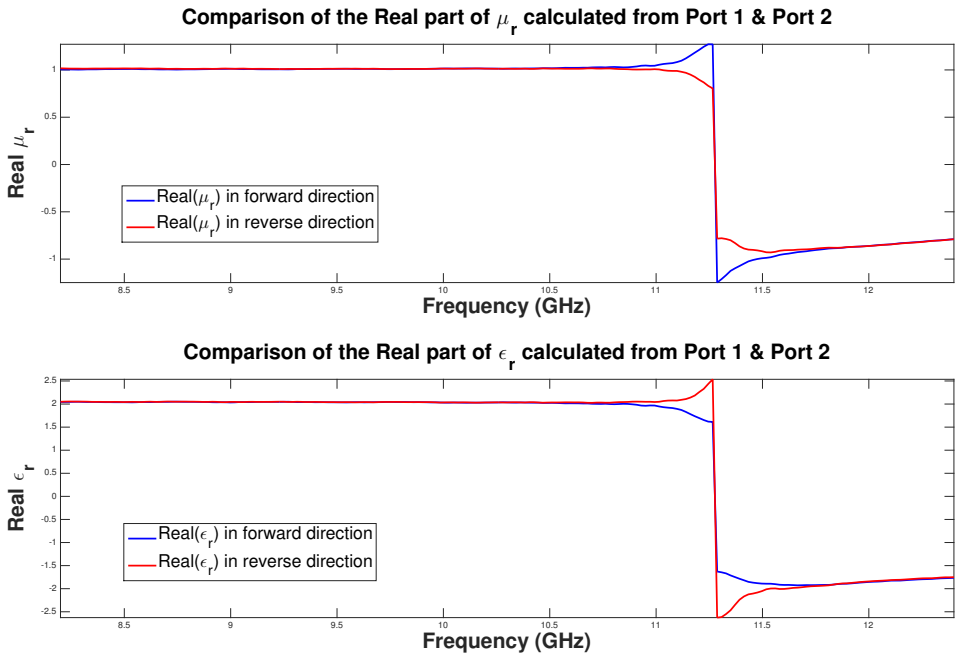

(a) Above: BA Sample 3 - Occlusions oriented to create XX-oriented $\vec{E}$ field

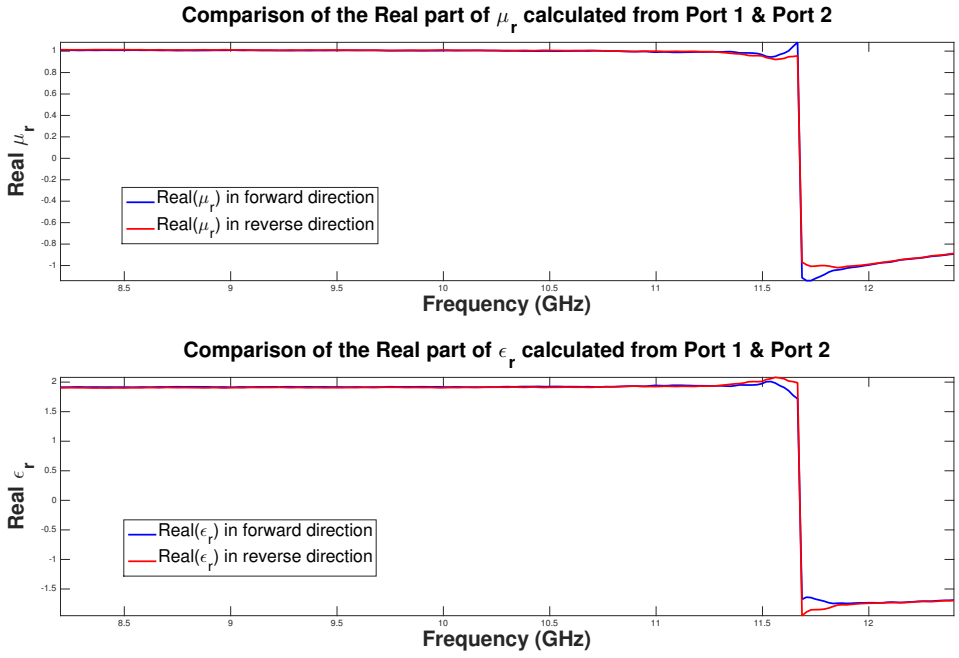

(b) Above: BA Sample 3 - Occlusions oriented to create YY-oriented $\vec{E}$ field

Figure 14. Biaxial sample 3 evaluated with NRW technique but no Newton root search

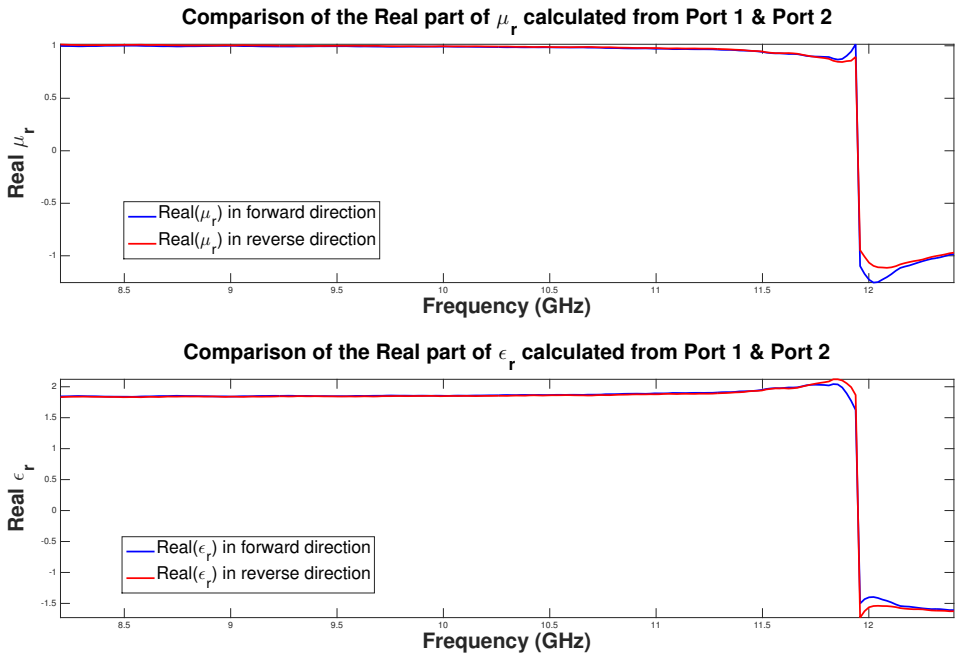

(a) Above: Uniaxial Sample - Occlusions oriented to create transverse $\vec{E}$ field

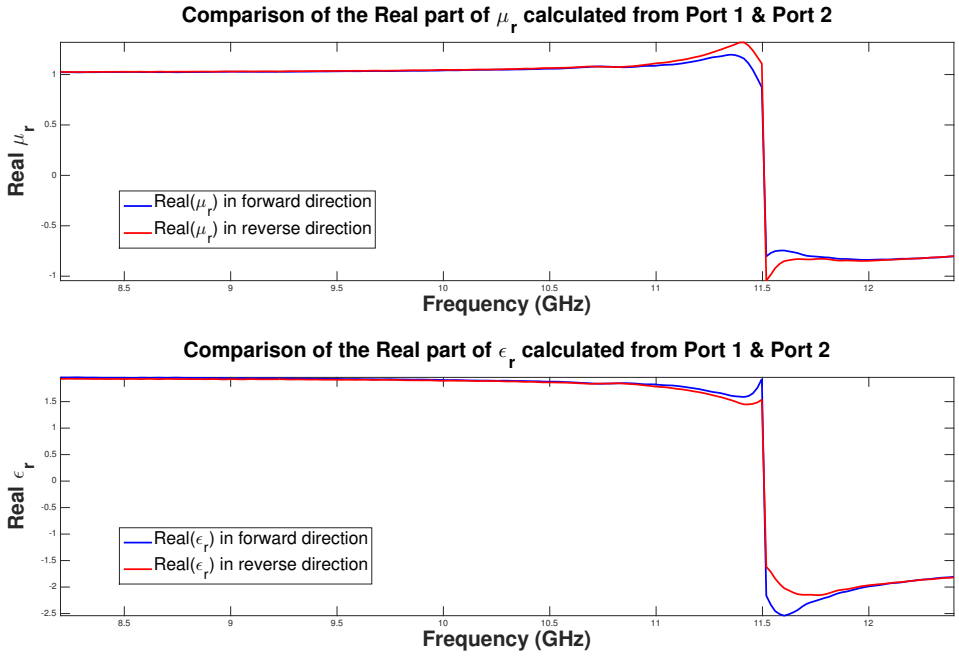

(b) Above: Uniaxial Sample - Occlusions oriented to create ZZ-oriented $\vec{E}$ field

Figure 15. Uniaxial sample evaluated with NRW technique but no Newton root search

The next pair of plots in Figure 16a-16b shows a representative example of what a layered system looks like after being run through the same NRW code as all the previous standalone samples. The data is clearly nonsensical, as the magnitude is negative, the μ data shows a significant and clear trend, and the ϵ data appears to blow up at the upper end of the X-band frequencies. Any useful data for the individual layers or total system is obfuscated by the inadequacy of applying the NRW method to a layered system.

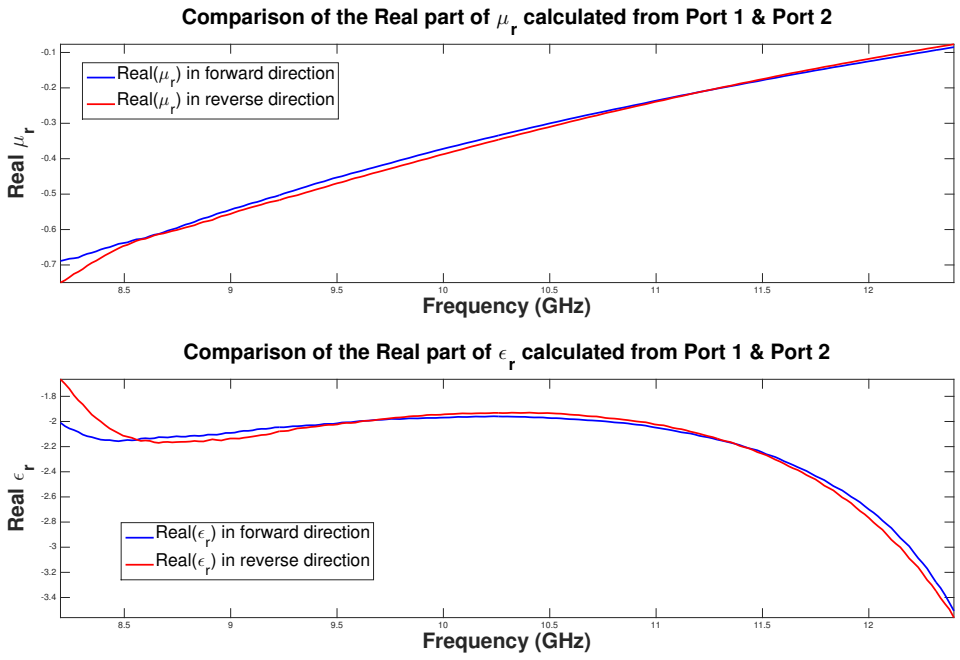

(a) Plexiglass|BA Sample 1 in XX orientation

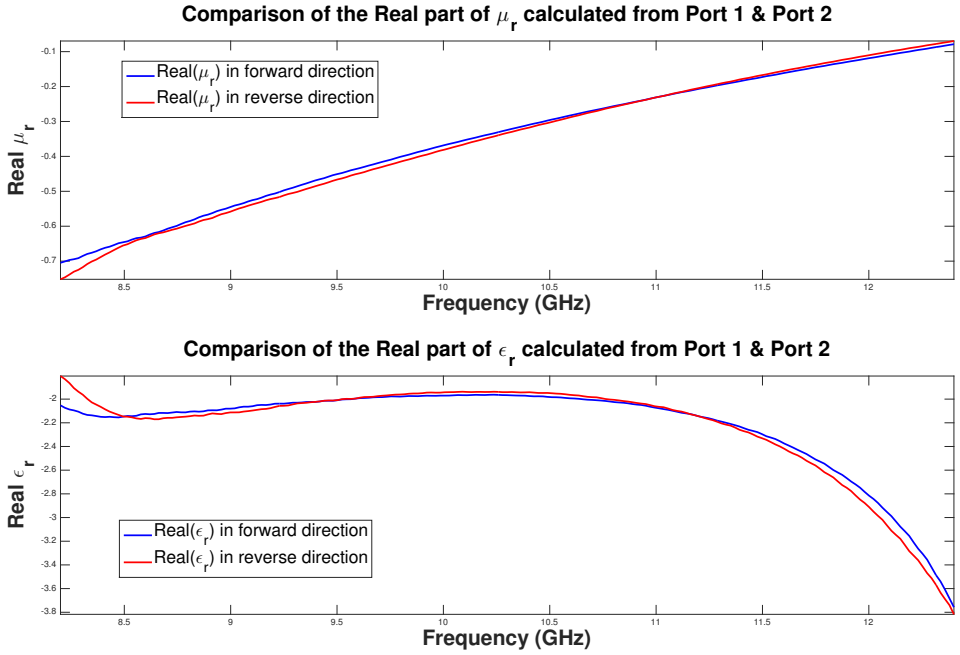

(b) Plexiglass|BA Sample 1 in ZZ orientation

Figure 16. Layered system of plexiglass and BA sample 1 evaluated with NRW technique but no Newton root search or layer extraction

Therefore, to overcome these undesirable effects, remove the discontinuity noted in the standalone plots in Figures 12-15, and characterize the biaxial layers, the code employing the Newton root search and layer extraction is applied.

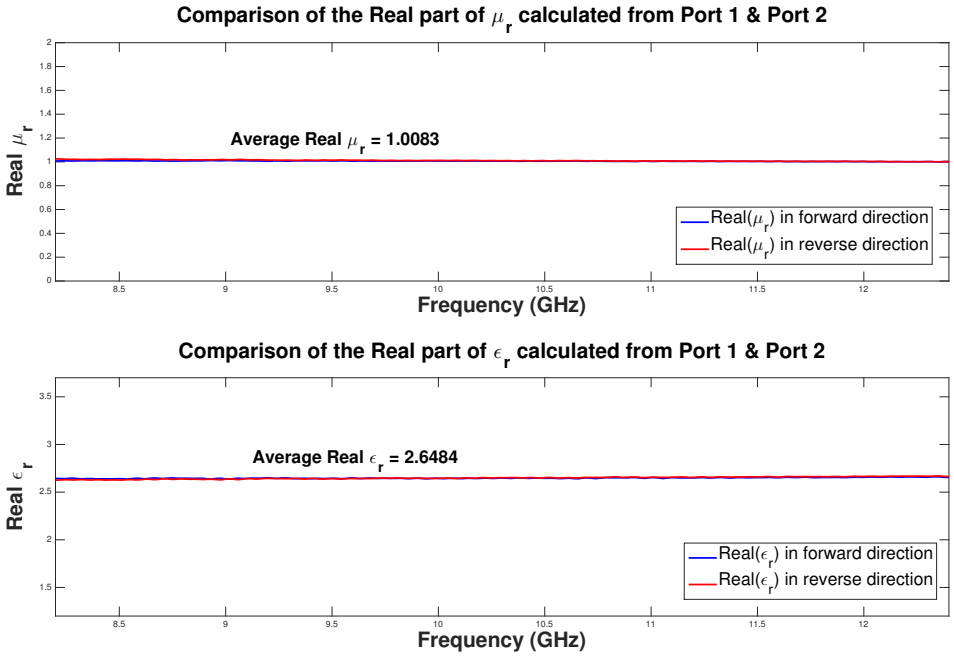

(a) Above: Plexiglass sample evaluated with NRW technique but no Newton root search

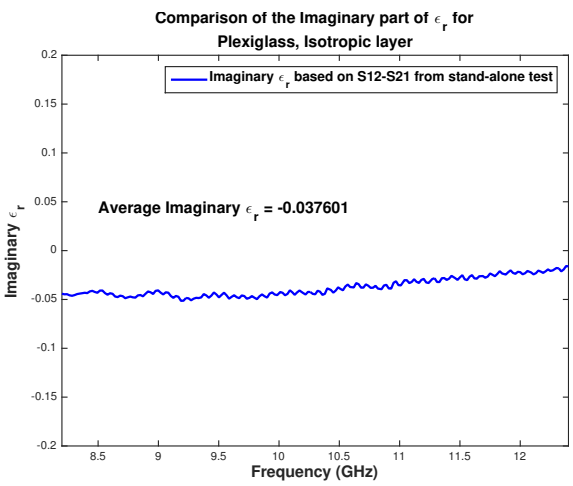

(b) Imaginary part of plexiglass sample evaluated with Newton Root Search

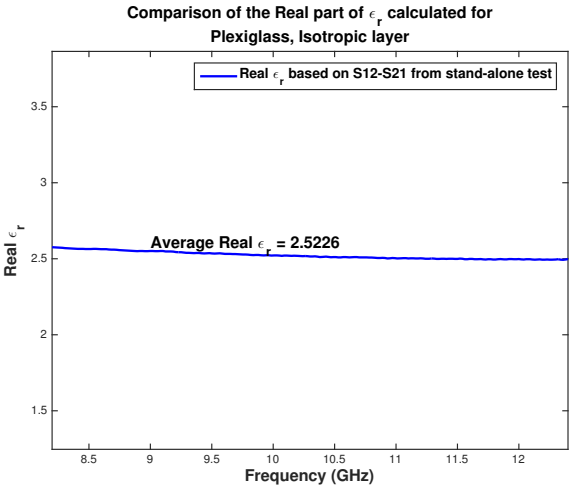

(c) Real part of plexiglass sample evaluated with Newton Root Search

Figure 17. Plexiglass sample standalone data comparison using two different methods

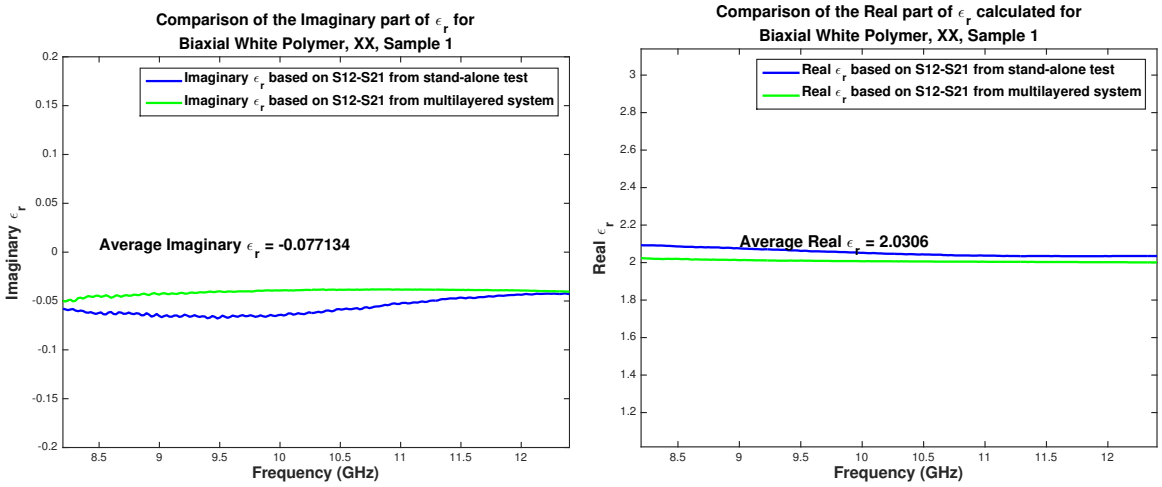

(a) Imaginary (b) Real

Figure 18. Layered system of plexiglass and BA sample 1 transverse(XX only), evaluated with Newton root search and layered extraction

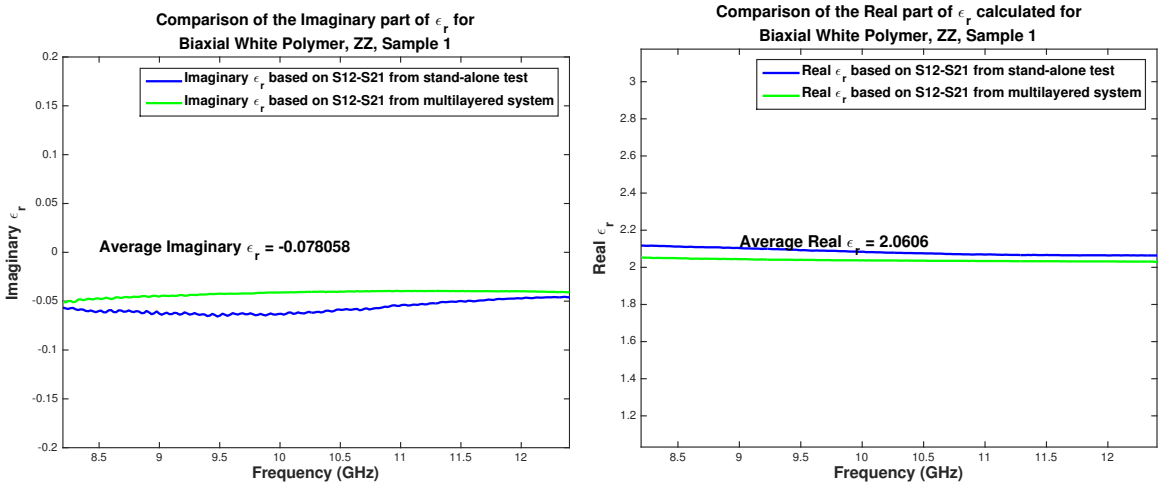

(a) Imaginary (b) Real

Figure 19. Layered system of plexiglass and BA sample 1 ZZ, evaluated with Newton root search and layered extraction

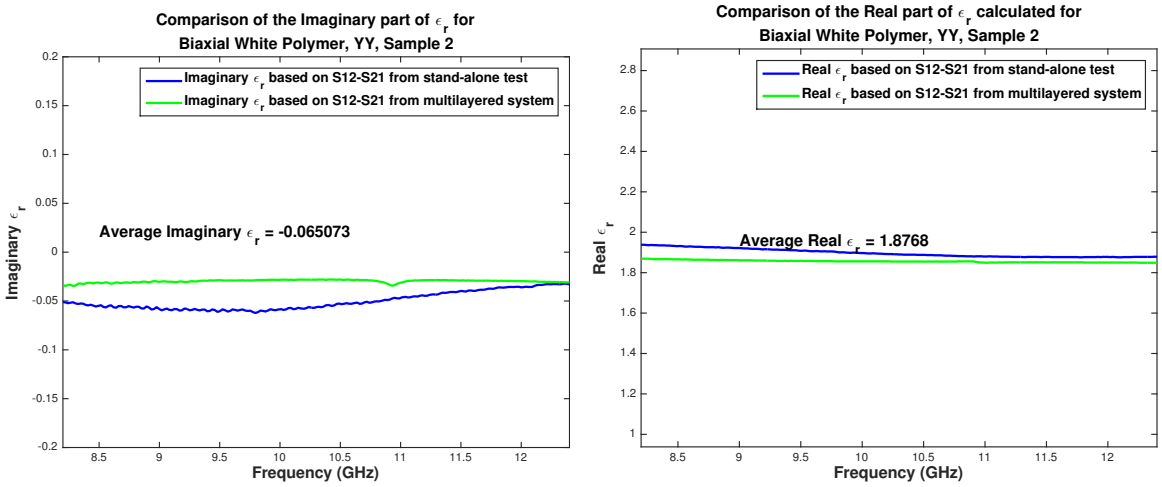

(a) Imaginary (b) Real

Figure 20. Layered system of plexiglass and BA sample 2 transverse(YY only), evaluated with Newton root search and layered extraction

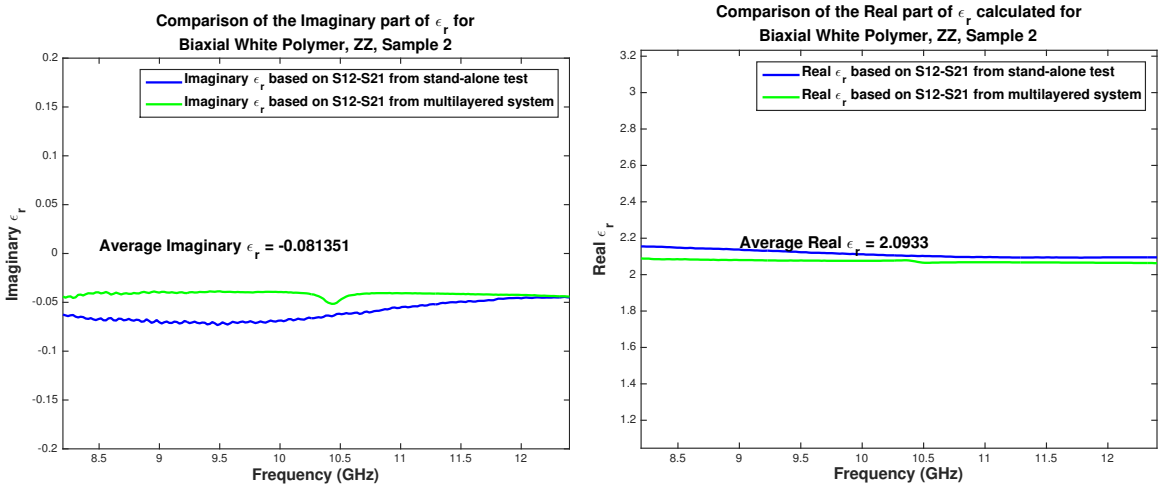

(a) Imaginary (b) Real

Figure 21. Layered system of plexiglass and BA sample 2 ZZ, evaluated with Newton root search and layered extraction

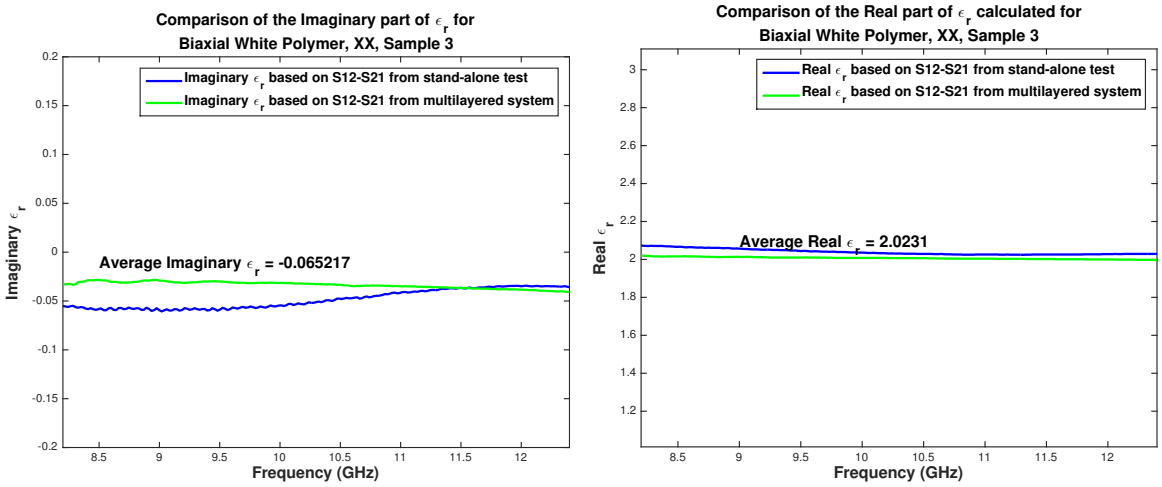

(a) Imaginary (b) Real

Figure 22. Layered system of plexiglass and BA sample 3 Transverse(XX only), evaluated with Newton root search and layered extraction

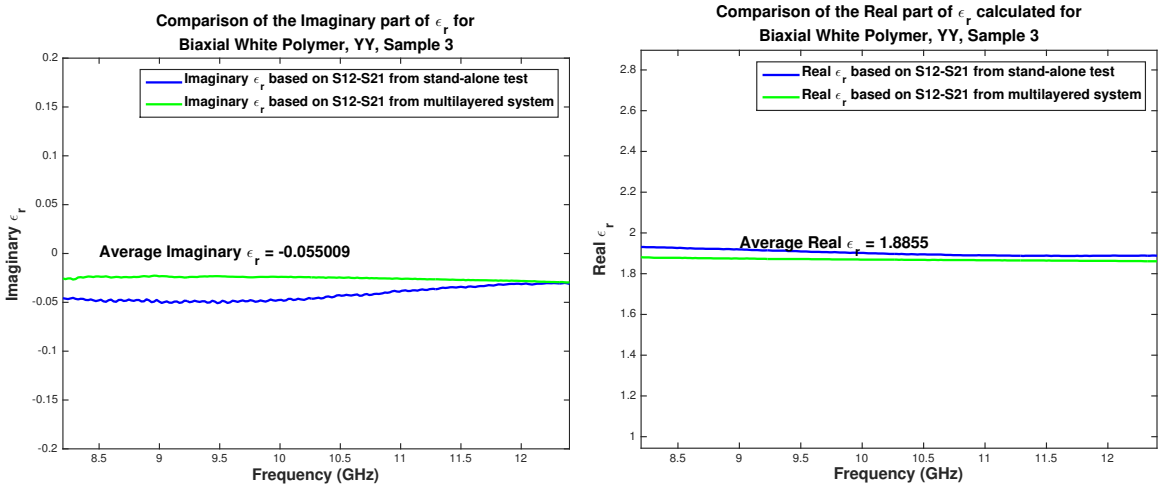

(a) Imaginary (b) Real

Figure 23. Layered system of plexiglass and BA sample 3 Transverse(YY only), evaluated with Newton root search and layered extraction

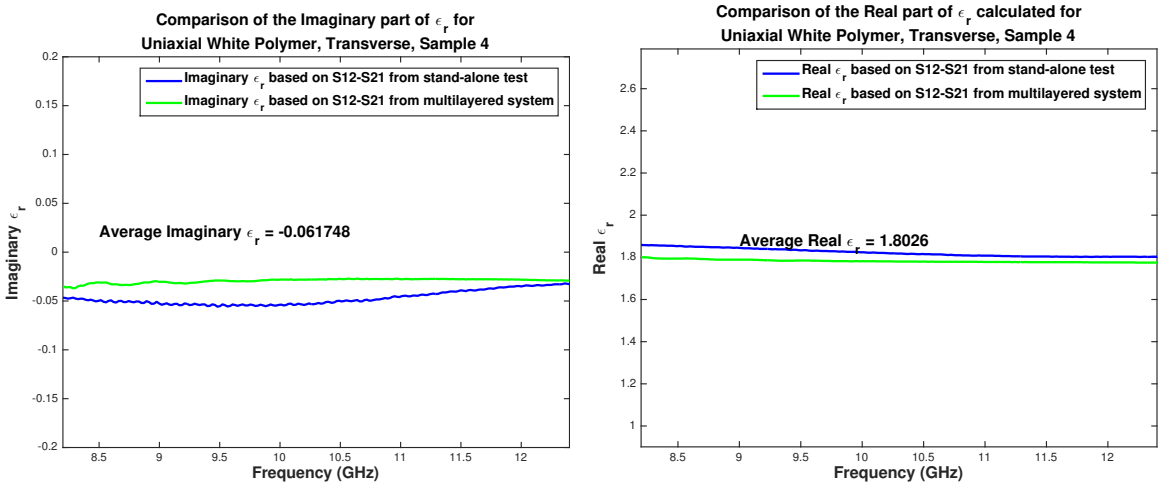

(a) Imaginary **(b) Real**

Figure 24. Layered system of plexiglass and uniaxial sample transverse, evaluated with Newton root search and layered extraction

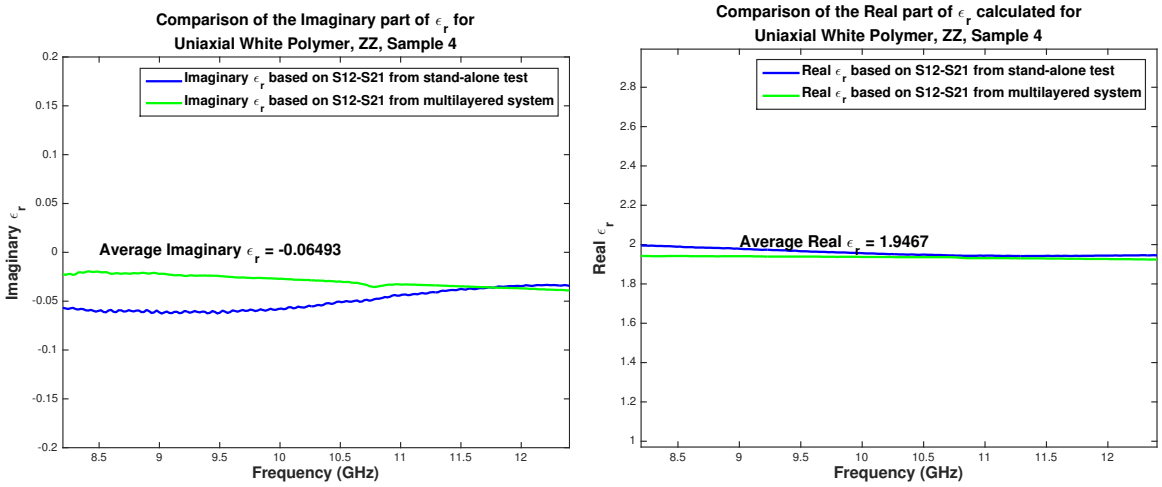

(a) Imaginary **(b) Real**

Figure 25. Layered system of plexiglass and uniaxial sample ZZ, evaluated with Newton root search and layered extraction

4.6 Explanation of Absence of Reflection Data .

It is noted in all of the results above that the measurements displayed in Figures 18-25 are based purely on transmission data, in other words, solving the second equation from Equation System 18, $S^{thy}_{21,sys}(\omega, \epsilon, \mu) - S^{exp}_{21,sys}(\omega) = 0$. This is due to the

sensitivity in the waveguide measurement system to sample location relative to Port 1 and 2 shown physically in Figure 26.

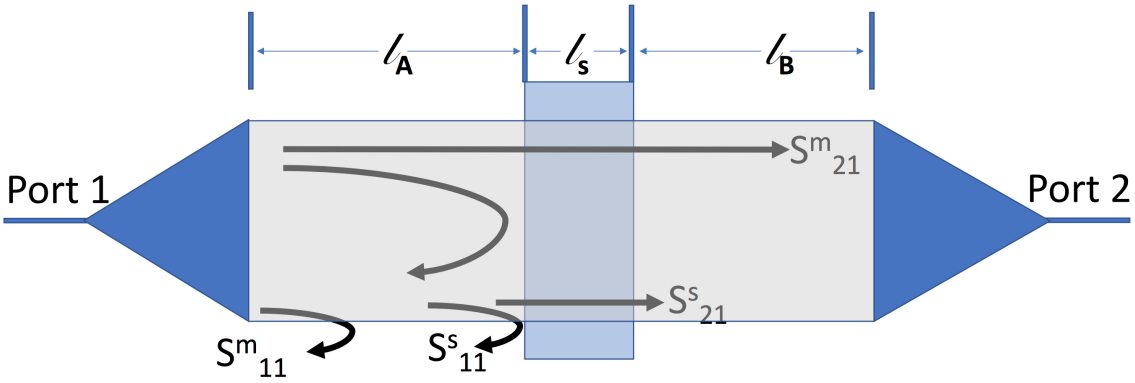

(a) Original experiment setup where:
- ℓ_A is the length from Port 1 to the left face of the sample,
- ℓ_s is the length of the sample,
- ℓ_B is the length from the right face of the sample to Port 2,
- S_{11}^m is the measured reflection from Port 1 at Port 1,
- S_{11}^s is the measured reflection from Port 1 at the sample plane,
- S_{21}^m is the measured transmission from Port 1 at Port 2,
- S_{21}^s is the measured transmission from Port 1 to Port 2 at the sample plane.

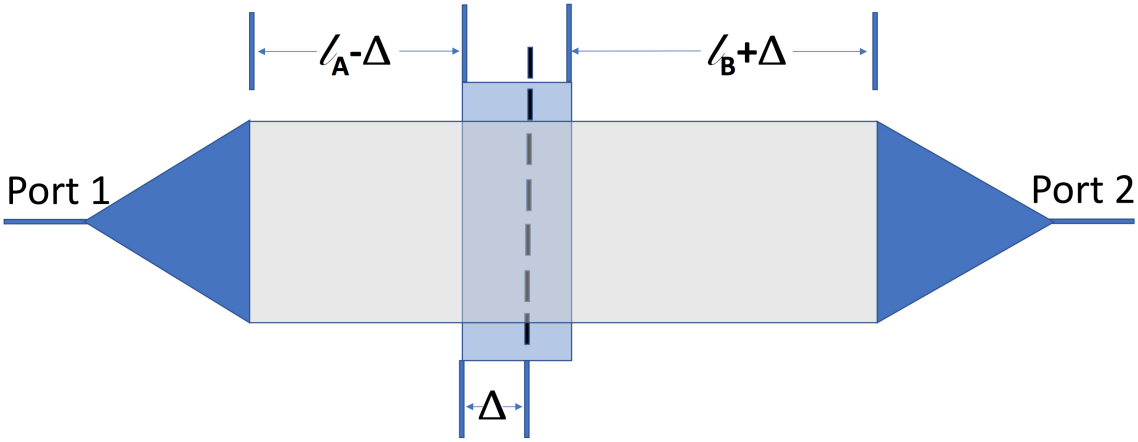

(b) Shifted experiment setup

Figure 26. A theoretical rectangular waveguide setup demonstrating the location-sensitivity of reflection S-parameters

The forward traveling waves for S_{11}^m and S_{21}^m can be described in terms of S_{11}^s and S_{21}^s respectively as

$$\begin{aligned} S_{11}^m &= S_{11}^s e^{-j2k_{z0}l_A} \\ S_{21}^m &= S_{21}^s e^{-jk_{z0}(l_A+l_B)} \end{aligned} \tag{24}$$

for the scenario in Figure 26a. These relationships are altered somewhat by the introduction of the phase shift in the reflection measurement induced by moving the system a distance Δ as shown in Equation system 25

$$\begin{aligned} S_{11}^m &= S_{11}^s e^{-j2k_{z0}(\ell_A-\Delta)} = S_{11}^s e^{-j2k_{z0}\ell_A}\mathbf{e^{j2k_{z0}\Delta}} \\ S_{21}^m &= e^{-jk_{z0}(\ell_A-\Delta)} S_{21}^s e^{-jk_{z0}(\ell_B+\Delta)} = S_{21}^s e^{-jk_{z0}(\ell_A+\ell_B)}. \end{aligned} \tag{25}$$

Furthermore, from NRW [2]

$$S_{11} = \frac{R(1-P^2)}{1-R^2P^2} \tag{26}$$

where $P = e^{-jk_z\ell_s}$, showing a dependence on the sample thickness for reflection measurements, which is an additional reason to refrain from using them calculate $\overleftrightarrow{\epsilon}$.

V. Conclusion & Future Work

5.1 Interpreting the Results.

This research is one part of an overall effort to further the ability to design and characterize anisotropic materials based on symmetry-based principles. The method employed in this thesis has been shown to be valid and novel in its application to biaxial anisotropic materials. The average percent difference between the single layer permittivity of the biaxial samples and that extracted for the same layer in the same orientation as part of a multilayer system was 1.9 %. Each BA sample's permittivity was found to vary from 0.1 - 0.7 % between orientations. This difference in permittivity is an artifact of the sub-wavelength occlusions acting as micro-capacitive elements where the longer dimension acts as a bigger capacitor when it is polarized by the TE_z fields. Finally, at lower frequencies within the X-band the difference in permittivity for the same sample between two orientations was slightly larger on average(1.12 %) than at the higher end of the band.

The percent difference between the permittivity measurements of each material (standalone vs layer extraction) are shown in Table 2, while the material tensors are fully reported in Table 3.

Material	**Orientation 1 (%)**	**Orientation 2 (%)**
Uniaxial sample	2.2 (transverse)	1.5 (ZZ)
Biaxial sample 1	2.0 (XX)	1.9 (ZZ)
Biaxial sample 2	2.6 (YY)	1.9 (ZZ)
Biaxial sample 3	1.5 (XX)	1.6 (YY)

Table 2. Percent difference of results for dielectric layered media permittivity extraction (real part) vs measured permittivty of a standalone sample

Material	Standalone Characterization	Single Layer Extraction from Multilayered System
Plexiglass sample	$\begin{bmatrix} 2.52 - j0.04 & 0 & 0 \\ 0 & 2.52 - j0.04 & 0 \\ 0 & 0 & 2.52 - j0.04 \end{bmatrix}$	None Performed
Uniaxial sample 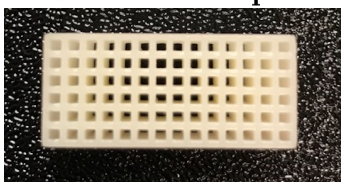	$\begin{bmatrix} 1.78 - j0.03 & 0 & 0 \\ 0 & 1.78 - j0.03 & 0 \\ 0 & 0 & 1.93 - j0.03 \end{bmatrix}$	$\begin{bmatrix} 1.82 - j0.05 & 0 & 0 \\ 0 & 1.82 - j0.05 & 0 \\ 0 & 0 & 1.96 - j0.05 \end{bmatrix}$
Biaxial sample 1 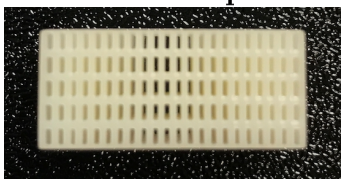	$\begin{bmatrix} 2.01 - j0.04 & 0 & 0 \\ 0 & \epsilon_{yy} & 0 \\ 0 & 0 & 2.04 - j0.04 \end{bmatrix}$	$\begin{bmatrix} 2.05 - j0.06 & 0 & 0 \\ 0 & \epsilon_{yy} & 0 \\ 0 & 0 & 2.08 - j0.06 \end{bmatrix}$
Biaxial sample 2 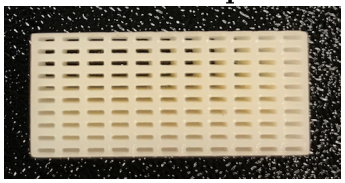	$\begin{bmatrix} \epsilon_{xx} & 0 & 0 \\ 0 & 1.85 - j0.03 & 0 \\ 0 & 0 & 2.07 - j0.04 \end{bmatrix}$	$\begin{bmatrix} \epsilon_{xx} & 0 & 0 \\ 0 & 1.90 - j0.05 & 0 \\ 0 & 0 & 2.11 - j0.06 \end{bmatrix}$
Biaxial sample 3 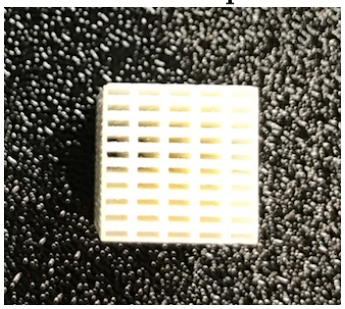	$\begin{bmatrix} 2.01 - j0.03 & 0 & 0 \\ 0 & 1.87 - j0.03 & 0 \\ 0 & 0 & \epsilon_{zz} \end{bmatrix}$	$\begin{bmatrix} 2.04 - j0.05 & 0 & 0 \\ 0 & 1.90 - j0.04 & 0 \\ 0 & 0 & \epsilon_{zz} \end{bmatrix}$

Table 3. Results for dielectric layered media permittivity extraction. The missing tensor element for each of the biaxial samples is the result of not being able to measure that orientation in a rectangular waveguide. If the goal were to fully characterize these samples, a WRWS would be required. All values are average values for each dataset

5.2 Future Work.

5.2.1 Focused Beam.

The advantages of taking the single layer extraction method into focused beam experiments are manifold. Chiefly, focused beam experiments would provide the ability to rotate samples into any orientation, as the focused beam apparatus is not restricted by an inherent physical coordinate system as in a waveguide. This would give rise to useful studies of cross polarization effects caused by the interrogating EM beam propagating through each layer at oblique angles. Such experiments would be significantly more complicated as there is no closed-form solution for the analysis of these effects in free space and y-invariance could not be assumed as in the waveguide.

5.2.2 Square Waveguide.

Extending the work done in this thesis to the WRWS system is the logical next step as that system allows comprehensive characterization of single biaxial samples. As has been noted elsewhere in this thesis, due to the nature of BA samples, only two orientations can be fully characterized in the rectangular waveguide but if these samples were to be manufactured as cubes, or cubes constructed of the sample layers, they could be fully characterized in the WRWS.

5.2.1 Including $\overleftrightarrow{\mu}$ for Magnetic Materials.

A further area of study to include in both of the aforementioned experiments would be magnetic materials, specifically the polymer biaxial anisotropic samples used in this thesis doped with Nickel or aluminum in the occlusions. This would allow for more complex and robust control of all the characteristics desired from LO coatings such as magnitude, phase, and polarization control, especially with multiple layers of dielectric and magnetic materials.

Bibliography

1. A. Knisely, *"Biaxial anisotropic material development and characterization using rectangular to square waveguide,"* Air Force Institute of Technology, Wright-Patterson Air Force Base, OH, March 2015.

2. A. Nicholson and G.F. Ross, "Measurement of the intrinsic properties of materials by time-domain techniques," *IEEE Transactions on Instrumentation and Measurement*, vol. 19, no. 4, pp. 377-382, 1970.

3. W. B. Weir, "Automatic measurement of complex dielectric constant and permeability at microwave frequencies," *Proceedings of the IEE*, vol. 62, no. 1, pp. 33-36, 1974.

4. T. Blakney and W. Weir, "Comments on "Automatic measurement of complex dielectric constant and permeability at microwave frequencies"," *Proceedings of the IEE*, vol. 63, no. 1, pp. 203-205, January 1975.

5. J. Baker-Jarvis, E. Vanzura, and W. Kissick, "Improved technique for determining complex permittivity with the transmission/reflection method," *IEEE Transactions on Microwave Theory and Techniques*, vol. 38, no. 8, pp. 1096-1103, 1990.

6. N. Damaskos, R. Mack, A. Maffett, W. Parmon, and P. L. E. Uslenghi, "The inverse problem for biaxial materials," *IEEE Transactions on Microwave Theory and Techniques*, vol. 32, no. 4, pp. 400-405, 1984.

7. B. Crowgey, O. Tuncer, J. Tang, E. Rothwell, B. Shanker, L. Kempel, and M. Havrilla, "Characterization of biaxial anisotropic material using a reduced aperture waveguide," *IEEE Transactions on Instrumentation and Measurement*, vol. 62, no. 10, pp. 2739-2750, October 2013.

8. J. Tang, B. Crowgey, O. Tuncer, L. Kempel, E. Rothwell, and B. Shanker, "Characterization of biaxial materials using a partially filled rectangular waveguide," in *34th Annual Symposium of the Antenna Measurement Techniques Association Conference Proceeding*, pp. 437-442, October 2012.

9. A. Knisely, M. Havrilla, P. Collins, M. Hyde, J. Allen, A. Bogle, and E. Rothwell, "Biaxial anisotropic material characterization using rectangular to square waveguide," in *36th Annual Symposium of the Antenna Measurement Techniques Association Conference Proceeding*, pp. 437-442, October 2014.

10. M. Havrilla, M. Hyde, A. Bogle, "Improved bandwidth in rectangular waveguide material characterization measurements," in *36th Annual Symposium of the Antenna Measurement Techniques Association Conference Proceeding*, pp. 427-431, October 2014.

11. R. Collin, "A simple artificial anisotropic dielectric medium," *IEEE Transactions on Microwave Theory and Techniques*, vol. 6, no. 2, pp. 206-209, 1958.

12. C. Balanis, *Advanced Engineering Electromagnetic*, ser. CourseSmart Series. Wiley, 2012.

13. D. Pozar, *Microwave Engineering*. Wiley, 2004.

14. G. F. Engen and C. A. Hoer, "Thru-reflect-line: An improved technique for calibrating the dual six-port automatic network analyzer," *IEEE Transactions on Microwave Theory and Techniques*, vol. 27, no. 12, pp. 987-993, December 1979.

15. M. Havrilla and D. Nyquist, "Electromagnetic Characterization of Layered Materials via Direct and De-embed Methods," *IEEE Transactions on Instrumentation and Measurement*, vol. 55, no. 1, pp. 158-163, February 2006.

16. D. Rytting, "An analysis of vector measurement accuracy enhancement techniques," *RF and Microwave Symposium and Exhibition*, Hewlett Packard, March 1982.

17. ——, "Appendix to an analysis of vector measurement accuracy enhancement techniques," *RF and Microwave Symposium and Exhibition*, Hewlett Packard, March 1982.

REPORT DOCUMENTATION PAGE

Form Approved
OMB No. 0704–0188

1. REPORT DATE *(DD–MM–YYYY)*	2. REPORT TYPE	3. DATES COVERED *(From — To)*
23–03–2017	Master's Thesis	Sept 2015 — Mar 2017

4. TITLE AND SUBTITLE

Single Layer Permittivity Extraction from Multilayered Biaxial Anisotropic Media Using a Rectangular Waveguide

5a. CONTRACT NUMBER

5b. GRANT NUMBER

5c. PROGRAM ELEMENT NUMBER

6. AUTHOR(S)

Fogarty, Benjamin I., Capt, USAF

5d. PROJECT NUMBER

17G165

5e. TASK NUMBER

5f. WORK UNIT NUMBER

7. PERFORMING ORGANIZATION NAME(S) AND ADDRESS(ES)

Air Force Institute of Technology
Graduate School of Engineering and Management (AFIT/EN)
2950 Hobson Way
WPAFB OH 45433-7765

8. PERFORMING ORGANIZATION REPORT NUMBER

AFIT-ENG-MS-17-M-028

9. SPONSORING / MONITORING AGENCY NAME(S) AND ADDRESS(ES)

Air Force Research Labs, Sensors Directorate
Attn: Garrett Stenholm
2591 K Street, Bldg 254
WPAFB OH 45433-7602
DSN 904-6721, COMM 937-255-9179
Email: Garrett.Stenholm@afit.edu

10. SPONSOR/MONITOR'S ACRONYM(S)

AFRL/RYS

11. SPONSOR/MONITOR'S REPORT NUMBER(S)

12. DISTRIBUTION / AVAILABILITY STATEMENT

DISTRIBUTION STATEMENT A:
APPROVED FOR PUBLIC RELEASE; DISTRIBUTION UNLIMITED.

13. SUPPLEMENTARY NOTES

This material is declared a work of the U.S. Government and is not subject to copyright protection in the United States.

14. ABSTRACT

Electromagnetic characterization of layered biaxial media is a critical step in the design of modern low observable (LO) coatings, and with the advent of 3D printing technology it is now possible to design and create myriad different such materials. Biaxial materials are of specific interest due to the flexibility they provide for control over magnitude, phase, and polarization of the material system's response to interrogating electromagnetic (EM) energy. This research effort, rather than being concerned with the exhaustive characterization of a material, which has been previously done, is instead concerned with empirically proving a technique for extracting the constitutive parameters $\overleftrightarrow{\epsilon}$ and $\overleftrightarrow{\mu}$ of a specific biaxial material layer from experimentally measured scattering parameters of an entire multilayered biaxial material system. Towards this aim, a rectangular waveguide is used with several samples irradiated at X-band frequencies. The method explored in the research herein shows that the individual layers of a multilayered biaxial anisotropic dielectric material can be successfully characterized and extracted from the overall system, thus providing a valuable technique for characterizing complex layered material coatings.

15. SUBJECT TERMS

Electromagnetics, Rectangular Waveguides, RF Material Characterization, Anisotropic, Biaxial, Metamaterials

16. SECURITY CLASSIFICATION OF:			17. LIMITATION OF ABSTRACT	18. NUMBER OF PAGES	19a. NAME OF RESPONSIBLE PERSON
a. REPORT	b. ABSTRACT	c. THIS PAGE			Dr. Michael J. Havrilla, AFIT/ENG
U	U	U	U	54	19b. TELEPHONE NUMBER *(include area code)* (937) 255-3636, x4582; michael.havrilla@afit.edu